NASA
CR
3334-
pt.2
c.1

NASA Contractor Report 3335

Transient Dynamic Analysis of High-Speed Lightly Loaded Cylindrical Roller Bearings

II - Computer Program and Results

Thomas F. Conry and Peter R. Goglia

NASA

NASA Contractor Report 3335

Transient Dynamic Analysis of High-Speed Lightly Loaded Cylindrical Roller Bearings

II - Computer Program and Results

Thomas F. Conry and Peter R. Goglia
University of Illinois at Urbana-Champaign
Urbana, Illinois

NASA

National Aeronautics
and Space Administration

Scientific and Technical
Information Branch

1981

TABLE OF CONTENTS

SUMMARY

The governing differential equations of motion for a high speed

cylindrical roller bearing are programmed for numerical solution and

plotted output. This computer program has the capability of performing

a two-dimensional or three-dimensional simulation. Two numerical solu-

tions of the governing differential equations were obtained to simulate

the motion of a roller bearing, one for the two-dimensional equations of

motion and one for the three-dimensional equations of motion. Computer

generated plots were obtained and present such data as roller/cage

interaction forces, roller/race traction forces, roller/race relative

slip velocities and cage angular speed over a non-dimensional time

equivalent to 1.2 revolutions of the inner race. Roller axial displacement,

roller skew angle and skew moment are also plotted for the three-dimensional

solution. The trajectory of the cage center is plotted for both the two-

and three-dimensional solutions.

INTRODUCTION

The prediction of transient dynamic behavior of high speed cylindrical
roller bearings is necessary to evaluate new design concepts and design
changes in existing bearings. Many phenomena, such as cage-roller impacts
and roller-flange impacts, which limit bearing life or affect bearing per-
formance are of a transient nature and may not be predicted using steady
state simulations. The prediction of roller or cage stability must be
done using methods of transient dynamic analysis with the proper nonlinear
models. Part I [1] of this report presents the derivation of the equations
of motion necessary to do the transient dynamic analysis of roller bearings.

Over the last decade much attention has been focused on the problem
of rolling element bearing transient analysis. Walters [2] was one of the
first investigators to attempt the solution of the total bearing dynamics
problem with realistic lubrication models. He made the basic assumption
in his analysis that the ball-race elasticity analysis can be performed
independently prior to the dynamics analysis because the ball-race normal
forces are large and the other forces, i.e. traction, ball spinning, have
little influence on the ball-race force balance. This same assumption was
used in [1] and is programmed in this report. Walters used a fourth order
Runge-Kutta scheme to integrate the equations of motion in contrast to the
use of the multivalue method of Gear [3] for stiff systems which is used in
this report.

Gupta [4] has presented a series of papers which treat the dynamics of
both ball and cylindrical roller bearings. The force models utilized by Gupta
are essentially the same as used in this computer program. The formula-
tion of the differential equations, as programmed in this report, is different

2

from [4] and is discussed in [1]. A Runge-Kutta-Merson method was used to numerically integrate the differential equations of motion in [4] again in contrast to the use of the multivalue method of Gear [3] in this report.

The purpose of this research program was to develop computationally efficient models which describe the interactions among forces, relative velocities and relative displacements in a high speed lightly loaded cylindrical roller bearing and to program the resulting differential equations of motion for a digital computer to obtain numerical solutions to these differential equations. These objectives have been achieved and the resulting computer program is presented in subsequent sections of this report.

The section ORGANIZATION OF THE COMPUTER PROGRAM discusses each subroutine. The dependent variables are defined together with their ordering scheme.

The results of a two-dimensional and a three-dimensional simulation are presented in RESULTS to illustrate the use of the computer program. These output data are in the form of plots of quantities of interest such as roller-race traction forces and roller-cage impact forces. All the plotted output data are discussed in DISCUSSION OF RESULTS. The final section contains the CONCLUDING REMARKS. The Appendices contain detailed information on the input data and output data.

ORGANIZATION OF THE COMPUTER PROGRAM

The purpose of the computer program is to obtain a numerical solution to the governing differential equations of motion described in Part I [1]. These equations are represented as a system of first order nonlinear differential equations of the form

$$\frac{d\underline{y}}{dT} = \underline{f}\,(\underline{y},\, T) \tag{1}$$

where $\underline{y}$ is the vector of state variables

   T is the dimensionless time

   $\underline{f}$ is the vector function

The computer program is organized into three major parts: the main program which controls the input and output, the differential equation solver, and the subroutines which are used to evaluate the vector function $\underline{f}\,(\underline{y},\, T)$. Fig. 1 shows the interrelationship of all the subroutines in the computer program.

The multivalue method of Gear [3] was utilized in the development of the computer program. This method has been shown to be effective in the solution of stiff systems of equations. The predictor step is taken by extrapolating out to a new value of the state vector. The extrapolation function is a weighted combination of values of the state vector at previous times. The corrector step is based on the implicit method of solving differential equations.

The multivalue method proved to be successful and necessary when the problem of the roller impacting the cage and flange was introduced. The
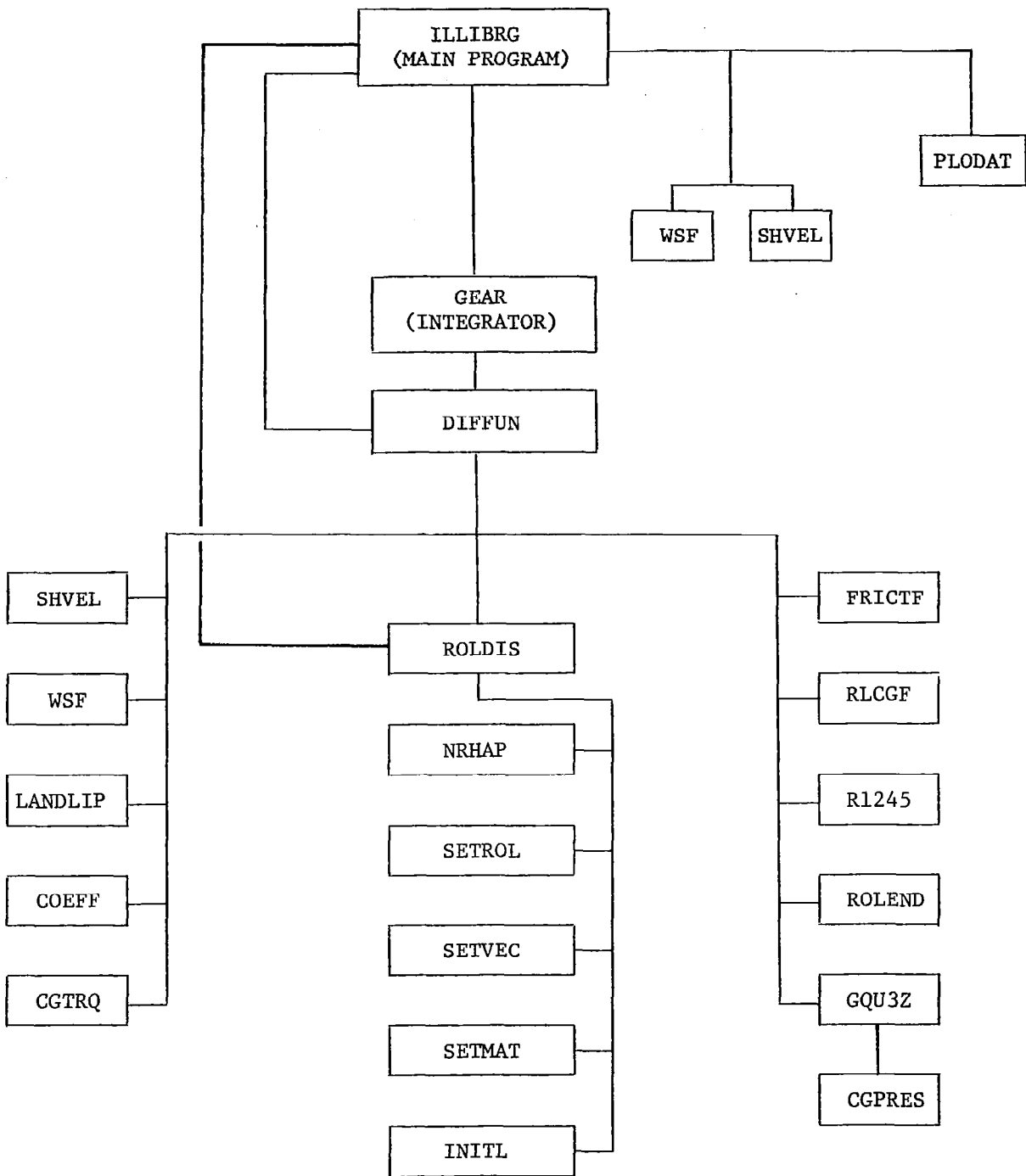
4

```
                    ILLIBRG
                (MAIN PROGRAM)                                    PLODAT

                                          WSF    SHVEL

                     GEAR
                  (INTEGRATOR)

                    DIFFUN


  SHVEL                                                    FRICTF

   WSF                  ROLDIS                             RLCGF

  LANDLIP               NRHAP                               R1245

  COEFF                 SETROL                             ROLEND

  CGTRQ                 SETVEC                             GQU3Z

                        SETMAT                            CGPRES

                        INITL
```

Figure 1:   Interrelationship of Subroutines
            to the Main Program - ILLIBRG

5

abrupt change in compliance upon impact causes the eigenvalues of the differential equations to change abruptly. These eigenvalues can range over several orders of magnitude when some rollers are under impact and others are not.

Each major subroutine in the computer program will now be discussed.

Program ILLIBRG

The purpose of the main program is to control the input and the output of the program and to call the differential equation solver. This program also calculates constants for use throughout the program and converts input quantities to other units which are more convenient for use in the program. The maximum and minimum allowable step sizes together with the specification of the total time over which the equations are integrated are controlled from this program.

The input is read in card-image form and includes the geometrical and inertial properties of the roller and the cage, the properties of the lubricant and the initial conditions of the bearing state vector y. The initial conditions on the first derivatives with respect to time are normally read in units of the epicyclic speed and are converted in the computer program to units of the speed ω_e as given in equation (73) of Part I [1].

The output of the program is the state vector y which is printed at time intervals subject to the user's option. Other data, including the roller traction forces, the relative slip velocities, the roller skewing moments and the trajectory of the cage center, are plotted from subroutine PLODAT, which is the most convenient way to present the large amount of output data. In addition to the plotting subroutine, files have been set up to store the output data of interest at a time interval set by the user. After the program

has terminated, the data stored on these files can be used as data in a special purpose plotting program to machine plot the data, or as input data for a subsequent run.

Differential Equation Solver

The differential equation solver used was the multivalue value method for stiff systems programmed in GEAR. This subroutine is called by the main program with a desired step size. The subroutine GEAR and its subsidiary subroutines perform the integration for the desired step size and returns to the main program where the time variable is updated. The subroutine GEAR used in this program was developed at the Lawrence Livermore Laboratory [5].

Subroutine for Plotting Data

Operational data generated by the computer program is plotted according to the instructions in subroutine PLODAT. The data plotted by this subroutine are the net circumferential forces on the roller, the traction forces at the inner and outer races, the roller to race relative slip velocities at the inner and outer race, the ratio of the cage angular velocity to the epicyclic speed and the trajectory of the cage center. Additionally, for the three dimensional problem, the roller axial displacement, the roller skew and the skew moment due to traction force distribution between the roller and the races are plotted.

Title blocks are inserted on each plot and are specific to the problem being solved. The plot statements used in PLODAT are specific to the Illinois Calcomp ® Graphics system and would have to be modified to fit the plotting systems of other computer installations.

7

The plot data are stored in arrays in the main program, ILLIBRG, in two dimensional array form. After the integration has been completed, these data are rearranged and packed into one dimensional arrays with two blank spaces separating the data for each roller. These spaces are used to store the scaling factors needed to plot the data in subroutine PLODAT.

Subroutine for the Differential Equation Solver

Subroutine GEAR requires a subroutine to calculate the vector function f (y, T) in equation (1). This subroutine is named DIFFUN.

Subroutine DIFFUN calculates many of the forces and torques acting in the roller bearing system. All the remaining subroutines are called directly or indirectly by DIFFUN in the calculation of the vector function f (y, T), Fig. 1.

Subroutine SHVEL

Subroutine SHVEL takes the user supplied values of total shaft linear deflection, the shaft rotation speed, the total angle of misalignment between the inner race and the outer race and whether the linear deflection and/or the angular misalignment is rotating or steady. This subroutine returns values of the linear deflections of the shaft in the x and y directions and the angular misalignments measured about the x and y axes as a function of time. The overall computer program, as it is now written, can only utilize SHVEL if the shaft speed is constant. If studies are to be made for an accelerating bearing, the equation

$$\theta_{shaft} = \int_0^T \omega_{shaft} (T) \, dT \qquad (2)$$

8

would have to be solved using GEAR and the value of θ_{shaft} would be required as input to SHVEL together with the time varying value of ω_{shaft}.

Function WSF

The function WSF is designed to give the shaft angular speed as a function of time. Presently the function is programmed to have a constant speed with time, but any speed-time relationship may be programmed. If the effect of a variation of shaft speed is desired, equation (2) would have to be programmed in DIFFUN and the result, θ_{shaft}, would have to be included as an input parameter to SHVEL.

Subroutine ROLDIS

Subroutine ROLDIS is called by ILLIBRG and DIFFUN. The method of Harris [6] and Liu [7] is programmed in this subroutine and its subsidiary routines. The geometry of the roller and the external displacements of the inner race with respect to the outer race are inputs to this subroutine. ROLDIS then organizes this information and returns with the static load distribution on each of the rollers.

Subroutine SETROL

SETROL computes the deviations of the roller surface from a pure cylinder due to crowning. The vector of variables, C_k, (refer to equation (8), [1]) at the center of each slice is an output of this subroutine. The roller centrifugal force per unit cage speed (in rpm) squared is also calculated in this subroutine.

Subroutine SETVEC

SETVEC calculates the values of the sine, cosine and the sign of the

cosine of the angles corresponding to the positions of the rollers in the bearing.

Subroutine INITL

This subroutine provides an initial set of values for the β_j's and the δ^o_j's in the solution of the nonlinear algebraic system of equations in ROLDIS. This subroutine is only called once; on the second and later calls, the previous solutions are used as the initial values for the iteration scheme.

Subroutine SETMAT

SETMAT sets up the Jacobian matrix for the Newton-Raphson iteration for the roller load distribution calculation. This routine is called at every iteration.

Subroutine NRHAP

This subroutine controls the Newton-Raphson iteration for the load distribution on the rollers. The systems of (2 X 2) equations are solved and the resulting incremental changes of the dependent variables are compared with the lower limit. If the changes are less than 10^{-5}, the iteration process is assumed to have converged.

Function COEFF

The correlation equation which relates the rolling velocity, sliding velocity, contact pressure and viscosity of the lubricant to the parameters necessary to obtain the traction coefficient is programmed in this function subroutine. The traction coefficient for the oil film between the roller and the races is the output of COEFF. The equations (20) - (23) of Part I [1] are programmed in COEFF.

Subroutine RLCGF

The regression equations for the dimensionless normal forces between the roller and cage are programmed in RLCGF. These equations are taken from Dowson, Markho and Jones [8].

Subroutine FRICTF

The regression equations from [8] for the dimensionless tractive forces between the roller and the cage are programmed in FRICTF. The two outputs of this subroutine are the dimensionless tractive force on the roller and the dimensionless tractive force on the cage.

Subroutine R1245

The drag on the cylindrical surface of the roller is calculated in R1245. The output of this subroutine is the drag torque on the outer surface of the cylinder, T_{rcyl}. The expressions used in this subroutine are based on the models used by Rumbarger, et. al. [10].

Subroutine ROLEND

The drag torques on the ends of the roller as the roller turns about its own axis are calculated in ROLEND. The expressions in this subroutine are based on the models used by Rumbarger, et. al. [10].

Subroutine CGTRQ

The drag torque on the outer surface and sides of the cage are calculated in CGTRQ. The area of the outer surface of the cage is estimated to be the surface area of the equivalent cylinder less the area of the pockets for the rollers. The expressions in this subroutine are based on the models in [10].

Subroutine LANDLIP

This subroutine calculates the horizontal driving force and the driving torque on the roller as a result of shearing the lubricant between the roller end and the inner race guide flange. The axial clearance between a roller end and the guide flange is assumed to be equal on both sides for purposes of this calculation for both the two- and three-dimensional simulations. The outputs of this subroutine are a net driving torque on the roller T_{RLAND} and a driving force F_{HLAND}.

Subroutine GQU3Z

This subroutine performs a composite Legendre-Gauss quadrature using a 96-point formula. The function which is numerically integrated is the pressure between the cage and the inner race guide flanges due to hydrodynamic action. The output of this subroutine is net force on the cage due to this pressure.

Subroutine CGPRES

The pressure function which is utilized in GQU3Z is evaluated in this subroutine. A check is made in this subroutine to assure that only the positive pressures are integrated.

The Dependent Variables

The dependent variables in the computer program are in the array Y(J). The number of dependent variables for the two dimensional problem is 3(NZ)+6 where NZ is the number of rollers in the bearing. The first six elements of Y(J) are used to describe the state variables of the cage. The first two elements are the dimensionless velocity and displacement of

12

the cage in the x direction. The next two elements are the dimensionless velocity and displacement of the cage in the y direction. The fifth and sixth elements are the dimensionless angular velocity and angular displacement of the cage.

The next group of three variables (seventh, eighth and ninth) represents the dimensionless relative velocity and displacement between the cage and the first roller and the angular velocity of the first roller about its own axis. The following group of three variables is associated with the second roller and so forth until the state variables of all NZ rollers have been described.

The three dimensional problem requires an additional 3(NZ) variables which are concatenated to the original 3(NZ)+6 variables described above. The first group of three variables represents the skewing angular velocity, the angular displacement and the axial displacement of the first roller. The next (NZ -1) groups of three variables represent corresponding quantities for the remaining (NZ -1) rollers.

13

RESULTS

The roller bearing dynamics program was utilized to illustrate the
dynamic behavior of an inner race guided high speed lightly loaded cylin-
drical roller bearing. The geometry of the bearing used in this investi-
gation is given in Table 1. The material of the rollers, races and the
cage is a conventional bearing steel. The relevant material properties
of the steel and the lubricant together with selected inertial properties
of the cage are given in Table 2. A steady state condition was obtained for
a two-dimensional simulation at a shaft angular speed of 70,000 revolutions
per minute with no misalignment and a rotating linear deflection of the shaft
of 0.020 mm, the state variables of which were used as the initial conditions
for the two cases analyzed in this report. These initial conditions on the
first derivatives   with respect to time were non-dimensionalized with
respect to the theoretical epicyclic speed eqn. (3).

$$\omega_{epi} = \frac{\omega_{shaft}}{2 \left(1 + \frac{r}{R}\right)} \tag{3}$$

where ω_{epi} is the theoretical epicyclic speed (radian/s)

ω_{shaft} is the shaft angular velocity (radian/s)

r   is the roller radius (mm)

R   is the radius of the inner race (mm)

The two-dimensional simulation was run for 1.2 revolutions of the inner
ring. The loading condition was a rotating linear deflection of the shaft
of 0.025 mm with no misalignment. The three-dimensional simulation was also
run for 1.2 revolutions of the inner ring with a loading condition of a
bearing misalignment of 0.002 radians and a steady shaft deflection in the y
direction of 0.020 mm.

14

The data obtained for the above two conditions are presented in Figures 2 through 18. The data presented for the two-dimensional case are the traction forces at the inner race and the outer race, the roller slip velocities at the inner race and outer race, the net circumferential forces between the rollers and the cage, the cage angular speed normalized on the theoretical epicyclic speed, and the trajectory of the cage center normalized on the radial clearance. The lines in the figures with multiple plots are labelled A through G corresponding to the seven rollers in the bearing.

The data presented for the three-dimensional case include the traction forces at the inner race and outer race, the net circumferential forces between the roller and the cage, the roller slip velocities at the inner race and outer race, the cage angular speed normalized on the theoretical epicyclic speed, the roller skew angle, the roller skew moment due to misalignments of the roller, and the dimensionless roller axial displacement. The input data corresponding to the two conditions described above are given in Tables 3 and 4. Appendix A, INPUT DATA, gives a detailed explanation of all the elements in these data sets.

TABLE 1

BEARING GEOMETRY

	(mm)
Bore	25
Inner Race Diameter	31
Guide Flange Height	2
Corner Radius, Inner Race Guide Flange	0.762
Outside Diameter	52
Outer Race Diameter	45
Roller Diameter	7
Roller Length	7
Crown Radius	635
Corner Radius of Roller	0.762
Cage Outside Diameter	42
Cage Inside Diameter	36
Cage Width	13
Roller/Cage Pocket Clearance, Circumferential	0.406
Roller/Cage Pocket Clearance, Axial	0.229
Pitch Diameter (Reference)	38
Diametral Clearance	0.025
Cage/Outer Race Diametral Clearance	4
Cage/Inner Race Guide Flange Diametral Clearance	0.356
Width of Guiding Lands/Cage Surfaces (2)	3
Roller/Inner Race Guide Flange Clearance	0.025

16

TABLE 2

MATERIAL, INERTIAL AND OPERATIONAL PARAMETERS

Bearing

Modulus of Elasticity; Roller, Cage, Races	2.0×10^{11} N/m^2
Poisson's Ratio; Roller, Cage, Races	0.30
Roller Weight	0.020 N
Density of Roller Material	7.75×10^3 kg/m^3
Polar Moment of Inertia of the Cage	7.71×10^{-6} kg-m^2
Cage Weight	0.176 N
Ratio of Oil Volume/Total Volume in Bearing	0.20
Number of Rollers	7

Lubricant (Mil-L-7808)

Absolute Viscosity	4.152 cp
Density	830 kg/m^3

TABLE 3

INPUT DATA AND INITIAL CONDITIONS FOR 2-D SIMULATION PRESENTED IN THE FORMAT DESCRIBED IN APPENDIX A

```
   7      8      2
30000000.  30000000.  30000000.      .30       .30       .30
   1.232      .2756      .001       .0005      .030      .030
    .2756    25.0         .004603  .72538000000000E-03
  .68213900000000E-04  1.398      .03961     .11470     .007      .016      .12
   4.151985    .03        .20
   0.00        0.00       .001       1.0
  70000.00
  .0002       0.00      1.20        .05
  .01
       -.9874705645D-01      .8191528305D+00      .4095124256D+00
       -.2213403995D+00      .8637317610D+00      .3615456008D+01
       -.2459280210D+00      .3704772010D+00      .4696269451D+01
        .1207631242D+01      .4919541581D+00      .4865091250D+01
        .3836438428D+00     -.1730080141D+00      .4810836815D+01
        .3601629631D-01     -.2337202076D+00      .4908954248D+01
       -.4948767425D+00      .4623993970D+00      .4801317850D+01
        .1092699572D+00     -.1780332250D+00      .4737511335D+01
        .1075714868D+00      .4433184912D+00      .4737316664D+01
        .2157924327D+03      .4899629083D+04
```

TABLE 4

INPUT DATA AND INITIAL CONDITIONS FOR 3-D SIMULATION PRESENTED IN THE FORMAT DESCRIBED IN APPENDIX A

```
   7      8      3
30000000.  30000000.  30000000.      .30       .30       .30
   1.232      .2756      .001       .0005      .030      .030
    .2756    25.0         .004603  .72538000000000E-03
  .68213900000000E-04  1.398      .03961     .11470     .007      .016      .12
   4.151985    .03        .20
   0.00        0.00       .001       1.0
  70000.00
  .0002       0.00      1.20        .05
  .01
       -.9874705647D-01      .8191528305D+00      .4095124257D+00
       -.2213403995D+00      .8637317611D+00    0.
       -.2459280210D+00      .3704772010D+00      .4696269452D+01
        .1207631242D+01      .4919541581D+00      .4865091250D+01
        .3836438428D+00     -.1730080141D+00      .4810836815D+01
        .3601629631D-01     -.2337202076D+00      .4908954249D+01
       -.4948767426D+00      .4623993970D+00      .4801317851D+01
        .1092699572D+00     -.1780332250D+00      .4737511335D+01
        .1075714868D+00      .4433184912D+00      .4737316665D+01
    0.                   0.                   0.
    0.                   0.                   0.
    0.                   0.                   0.
    0.                   0.                   0.
    0.                   0.                   0.
    0.                   0.                   0.
    0.                   0.                   0.
    0.                   0.                   0.
        .1328643991D+03      .3844584514D+04
```

18

DISCUSSION OF RESULTS

The results presented in this report are intended to illustrate the behavior of the computer program and to show the type of output data which may be obtained. The bearing used in these illustrative studies represents a high speed cylindrical roller bearing with the exception that the number of rollers was reduced from fourteen to seven. This was done to conserve computer time, as the primary purpose of this project was to develop a working computer program.

The effects of heat transfer were not considered in this project nor were they programmed in the computer code. The lubricant properties are specified as input data and they correspond to an operating temperature of the bearing. If a lubricant other than Mil-L-7808 oil is to be used, the function subprogram COEFF will have to be changed to provide the traction coefficient for the new lubricant.

Two-Dimensional Simulation

The two-dimensional simulation initial conditions and loading parameters represent the effect of a suddenly applied unbalance condition in an already unbalanced shaft. The maximum roller load increased from 591 N to 960 N. The effect of this sudden loading is shown in Figures 2 through 8.

The dimensionless normal cage forces acting on the rollers, FC, are plotted in Figure 2. The purpose of this plot is to show the time and location of cage roller impacts. A positive value of FC indicates that the cage is pushing the roller while a negative value indicates that the roller is pushing the cage. For most of the 1.2 inner ring revolutions the value of FC appears to be zero, but in fact is not. The components of FC are the normal approach hydrodynamic models and the Hertzian impact models. The magnitudes

70000 RPM   SHAFT DEFLECTION=0.025MM   MISALIGNMENT=0.0000RAD. 2-D MOTION
ROTATING DEFLECTION   STEADY MISALIGNMENT   MAX. ROLLER LOAD (N)=960.

Roller E

Roller F

Roller G

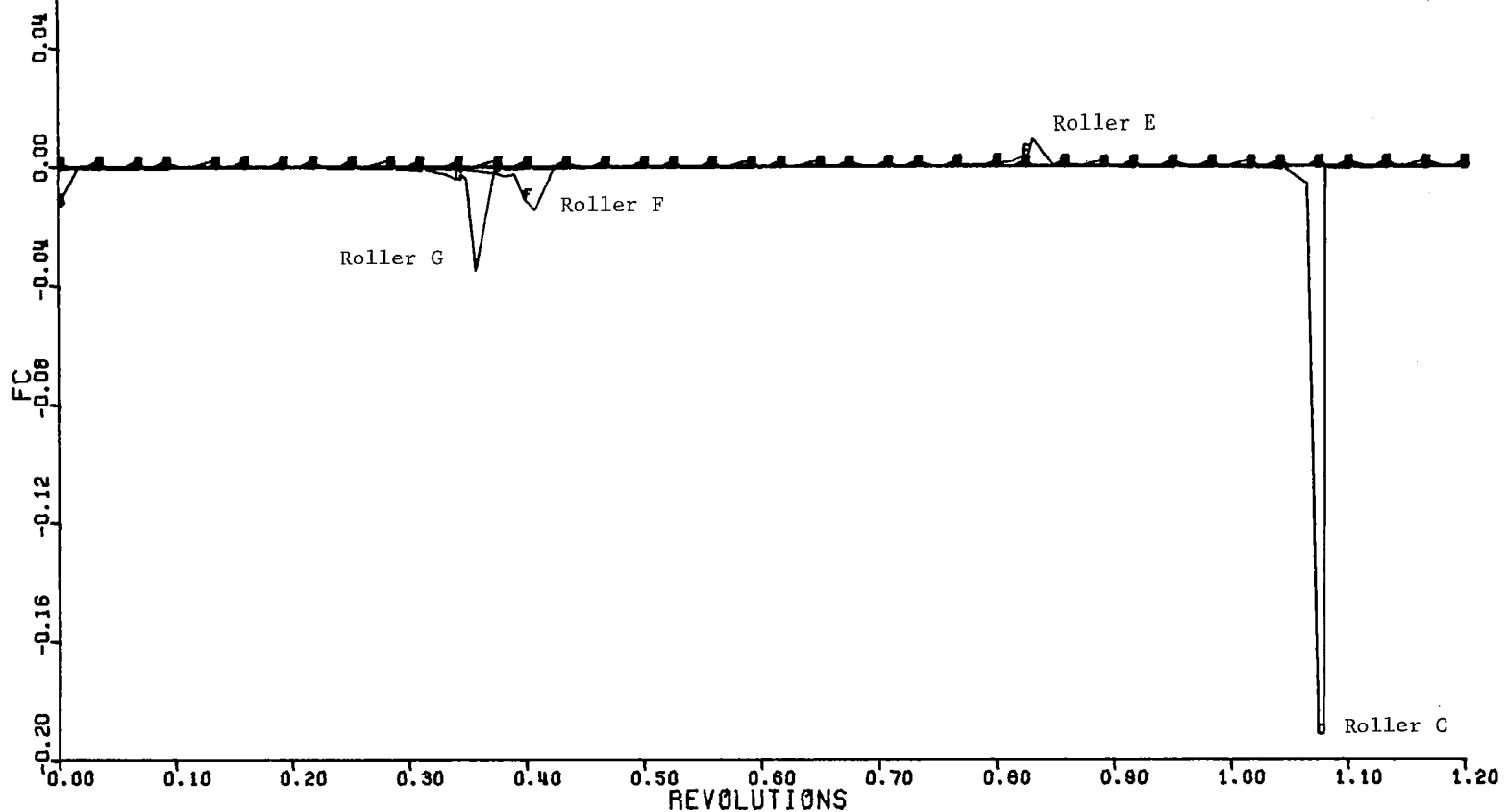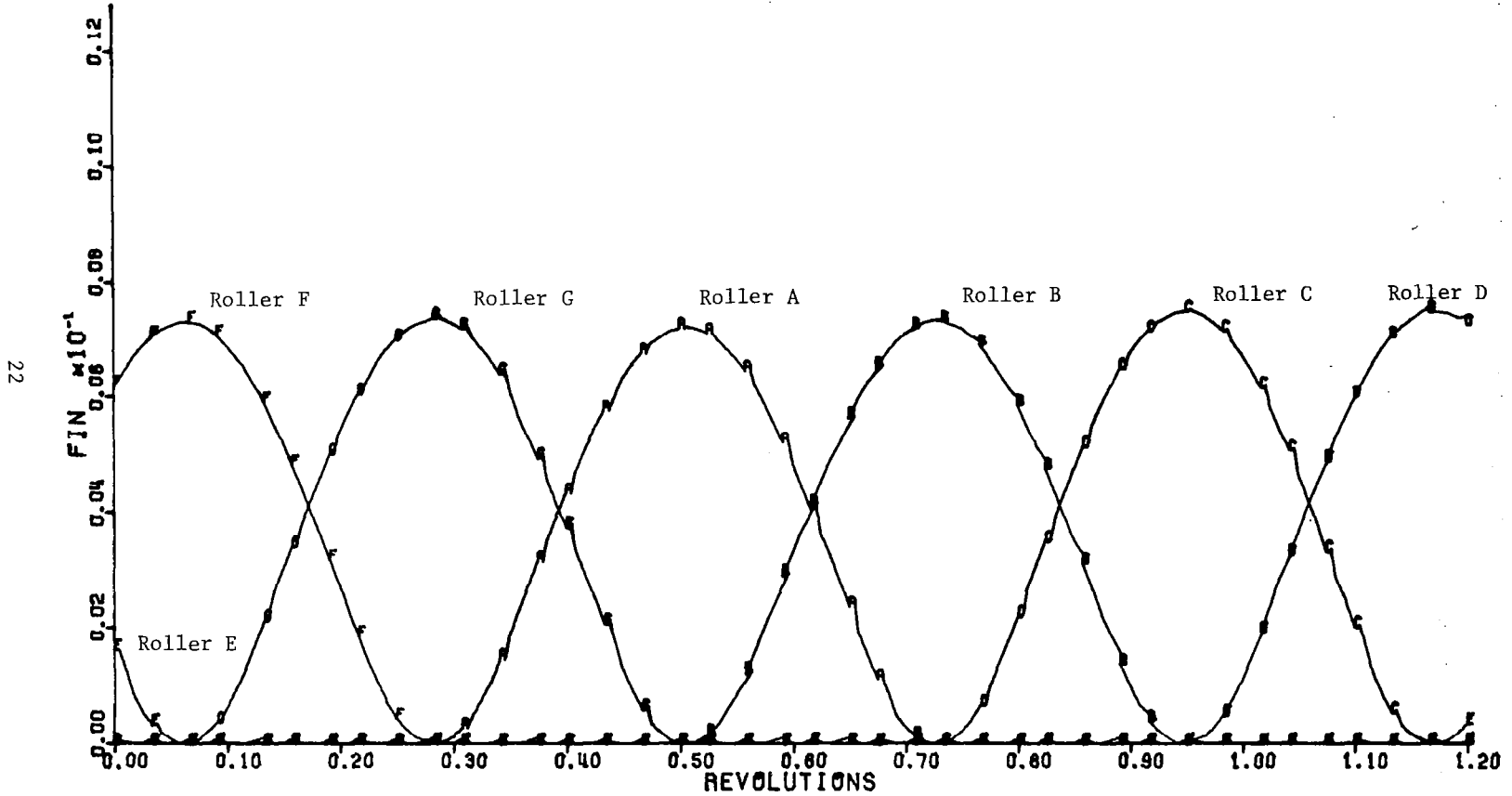Roller C

FC

REVOLUTIONS

Figure 2.   The Dimensionless Normal Cage Forces Acting on the Rollers for the 2-D Simulation Versus Time
          Measured in Revolutions of the Inner Race at 70,000 RPM

of the hydrodynamic forces are very small relative to those forces generated during Hertzian impact. When the data are scaled for plotting, the hydrodynamic forces will be plotted close to zero.

To examine the magnitude of the impact forces, consider the force between roller C and the cage at about 1.07 revolutions. The maximum impact force is $(.191)$ (960) = 183 N (41 lb_f). This force corresponds to a maximum Hertz stress between the cage pocket and roller C of 5.19×10^8 Pa $(75,225 \text{ psi})$.

The dimensionless traction forces on the rollers at the inner race, FIN, are plotted in Figure 3. The traction force is directly proportional to the normal force at the contact, which accounts for the periodic shapes as shown. In a high speed bearing, the rollers are usually pressed against the outer race due to the action of centrifugal force. Depending on the amount of diametral clearance, there is usually no contact between the roller and the inner race except in the load zone of the bearing. The time required for a roller to traverse this load zone is 0.44 revolutions of the inner race.

The magnitudes of the inner race/roller traction forces are small, about 7 N (1.58 lb_f), due to the low normal forces between the rollers and the inner race. The dimensionless outer race/roller traction forces, FOUT, however, achieve larger magnitudes, Figure 4. The magnitudes of these forces reach 48 N (10.8 lb_f).

70000 RPM   SHAFT DEFLECTION=0.025MM   MISALIGNMENT=0.0000RAD. 2-D MOTION
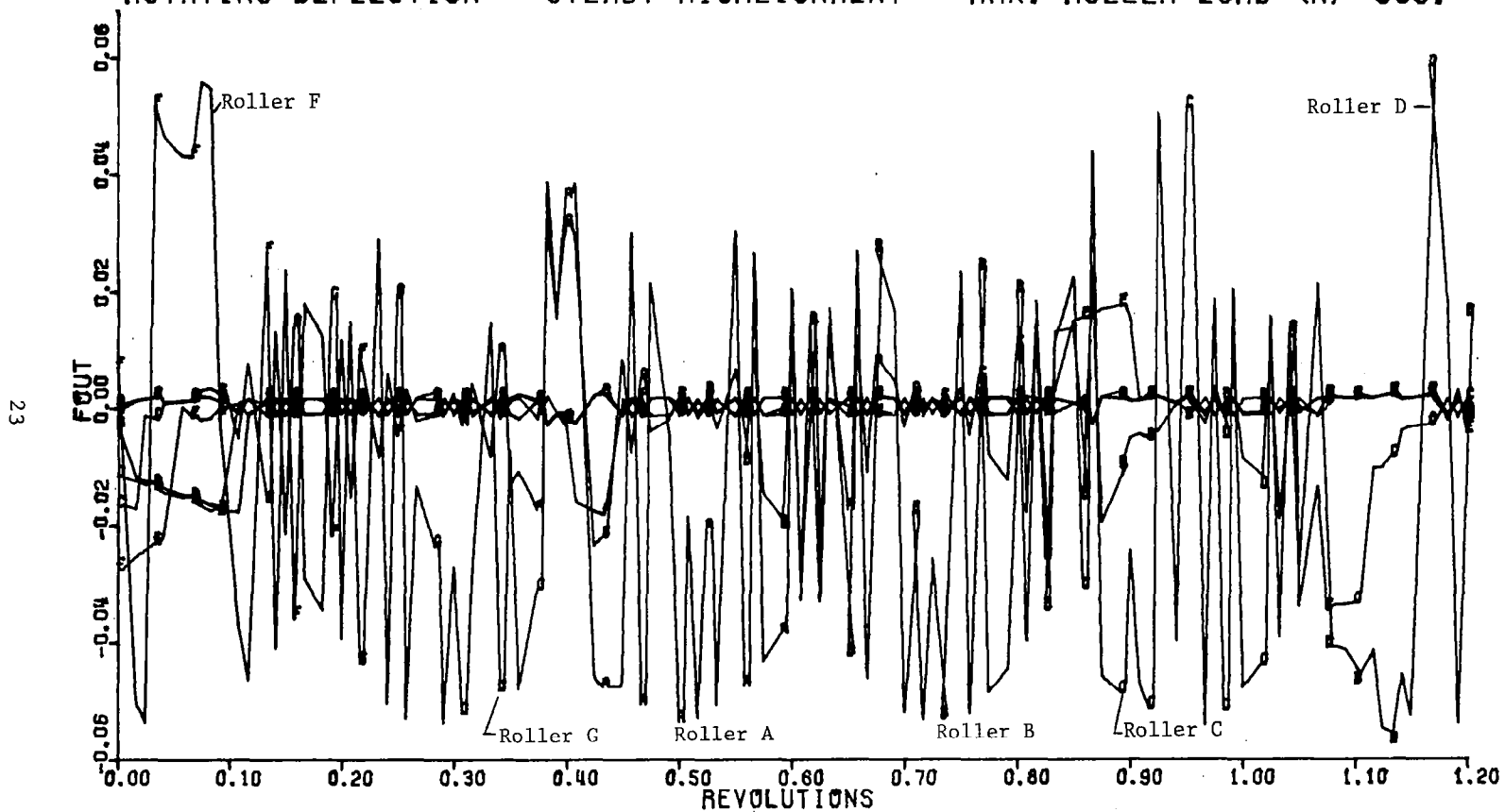ROTATING DEFLECTION   STEADY MISALIGNMENT   MAX. ROLLER LOAD (N) = 960.
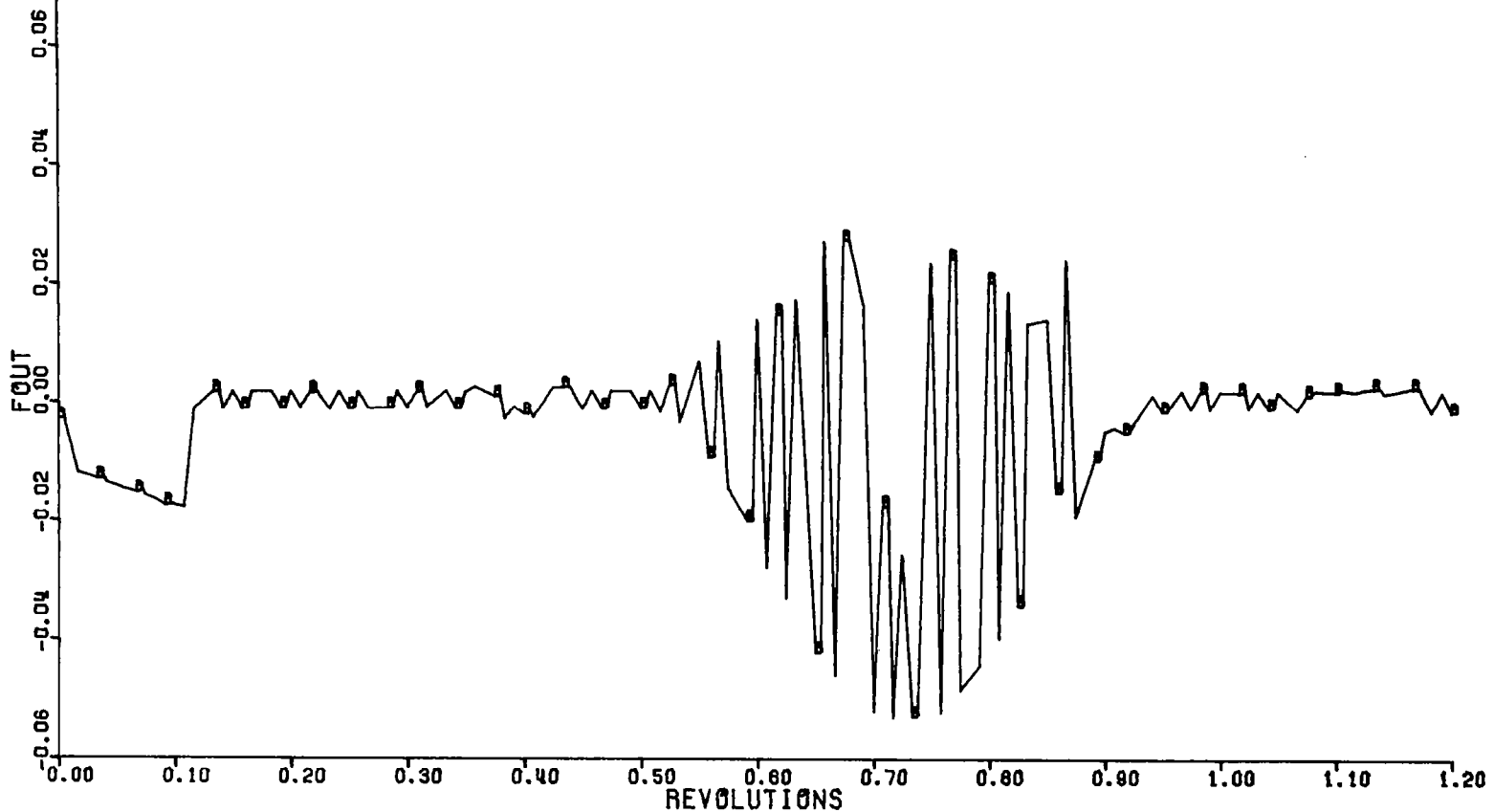

Figure 3.   The Dimensionless EHD Traction Forces on the Rollers at the Inner Race for the 2-D Simulation
Versus Time Measured in Revolutions of the Inner Race at 70,000 RPM

70000 RPM   SHAFT DEFLECTION=0.025MM   MISALIGNMENT=0.0000RAD. 2-D MOTION
ROTATING DEFLECTION   STEADY MISALIGNMENT   MAX. ROLLER LOAD (N)=960.

Figure 4a.   The Dimensionless EHD Traction Forces on the Rollers at the Outer Race for the 2-D Simulation
Versus Time Measured in Revolutions of the Inner Race at 70,000 RPM

70000 RPM   SHAFT DEFLECTION=0.025MM   MISALIGNMENT=0.0000RAD. 2-D MOTION
ROTATING DEFLECTION   STEADY MISALIGNMENT   MAX. ROLLER LOAD (N)=960.

Figure 4b.   The Dimensionless EHD Traction Force on Roller B at the Outer Race for the 2-D Simulation
Versus Time Measured in Revolutions of the Inner Race at 70,000 RPM

In the high speed bearing, the centrifugal force is significant and accounts for a large magnitude normal force between the rollers and the outer race around the circumference of the bearing. Since traction force is proportional to the normal force, the large magnitude of the traction force should be expected. Note that many of these dimensionless traction forces, FOUT, hover near zero (0 to 0.001). Note that the rollers undergoing the largest changes in traction forces are those rollers going through the load zone. This correlates with the results in Figure 3.

The relative slip velocities between the roller and the inner race, USIN, are plotted in Figure 5. Note that all the rollers have slip velocities between 12 and 16 m/s. These appear to be approaching an equilibrium condition and correspond to the traction forces required to equilibrate the rollers because of the small inner race/roller normal forces.

The relative slip velocities, USOUT, between the rollers and the outer race are shown in Figure 6. Note that all the slip velocities tend toward zero. This correlates with the values of the traction forces in Figure 4. The smallest deviation of relative slip velocity from zero is sufficient to cause a significant change in the traction forces FOUT. The non-zero values of USOUT in the first 0.10 revolutions of the inner race correspond to the set of initial conditions. At equilibrium, all values of USOUT should tend toward zero. The spikes in USOUT at 0.35, 0.40, 0.80, and 1.05 revolutions correlate with the impacts between roller and cage as shown in Figure 2. The first, second, and fourth events are the roller impacting the cage. This large impact force at the front of the roller tends to decelerate the roller in the path about the center of the bearing,

25

70000 RPM   SHAFT DEFLECTION=0.025MM   MISALIGNMENT=0.0000RAD. 2-D MOTION
ROTATING DEFLECTION   STEADY MISALIGNMENT   MAX. ROLLER LOAD (N)=960.
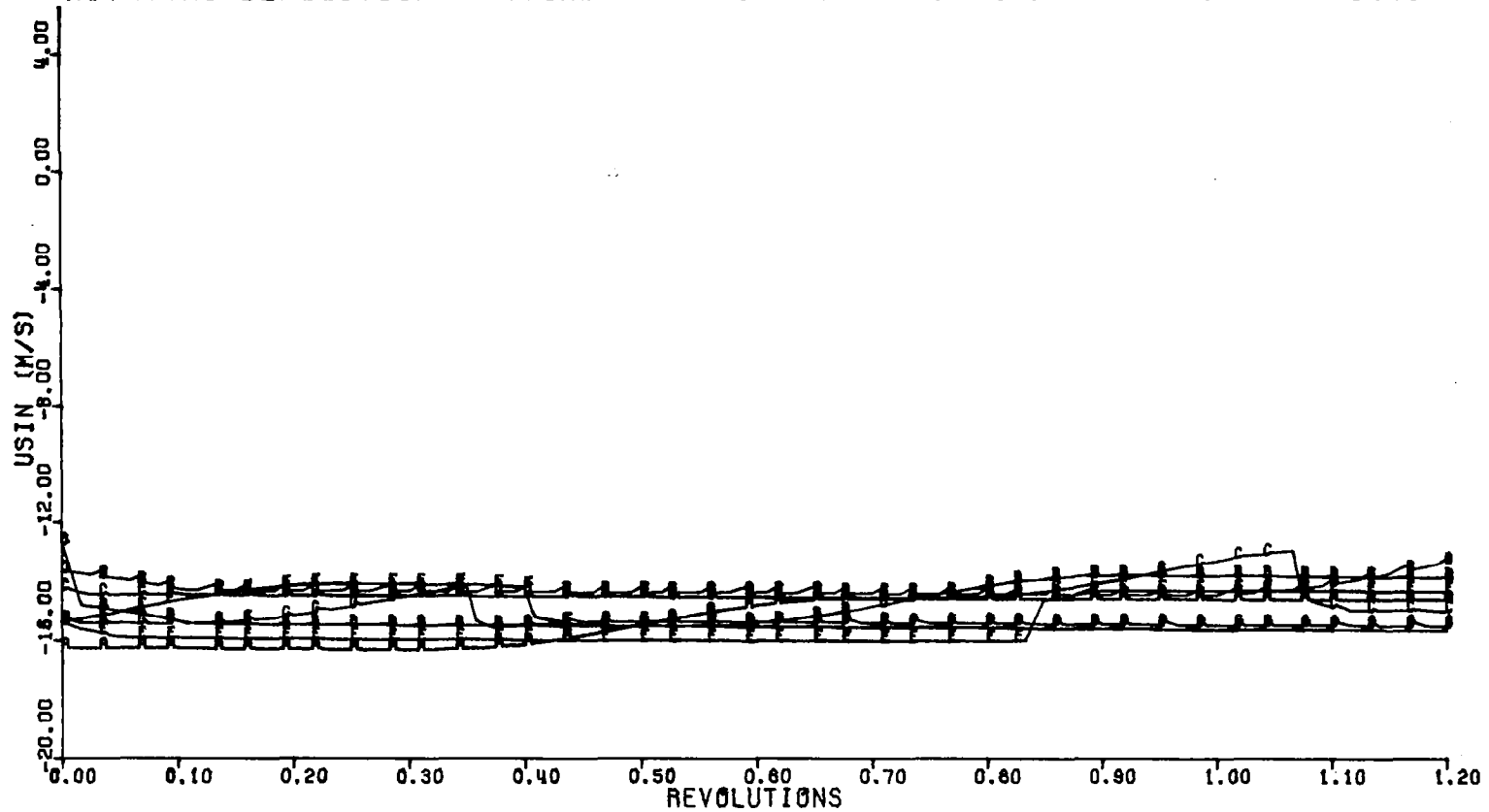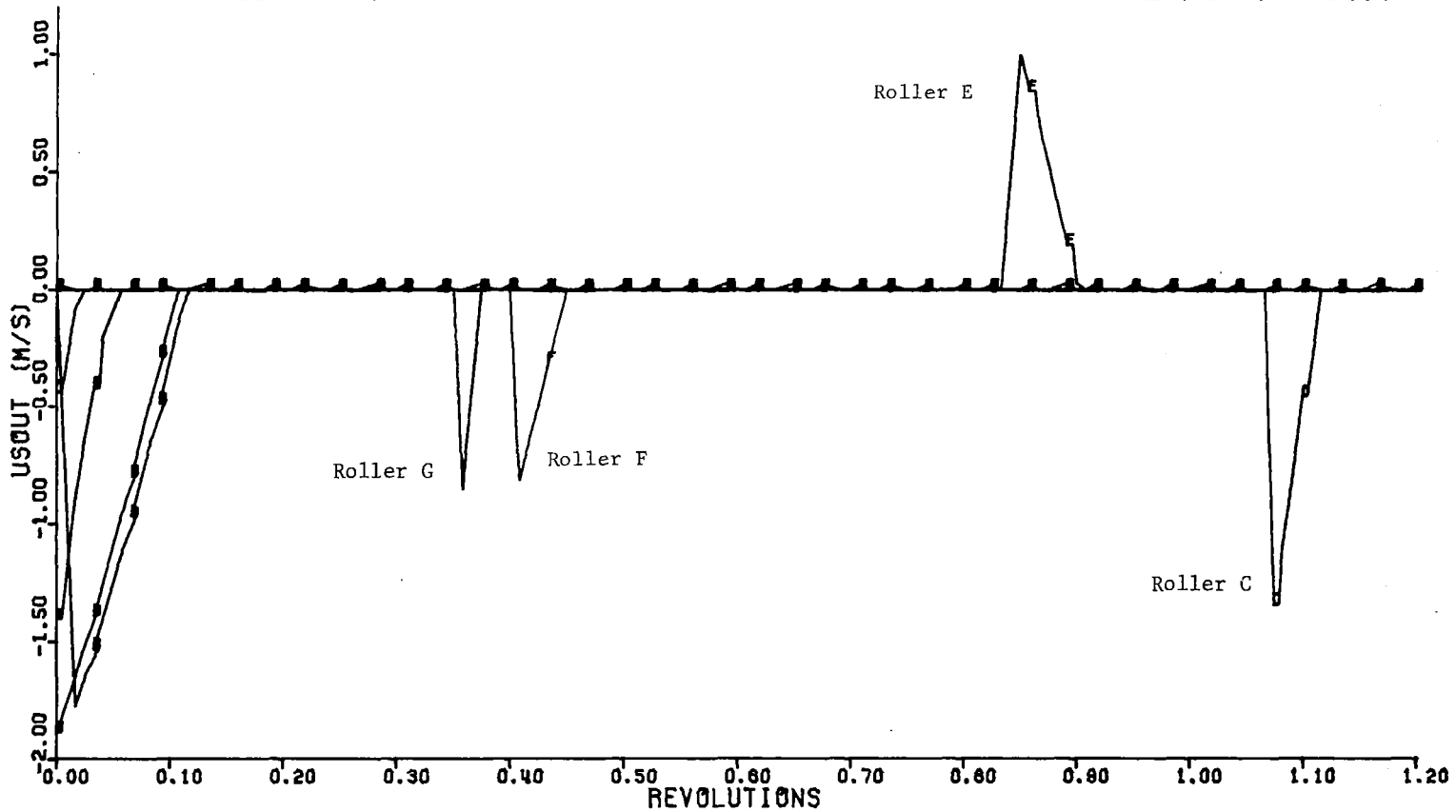
Figure 5.   The Relative Slip Velocities Between the Rollers and the Inner Race Versus Time Measured in
            Revolutions of the Inner Race at 70,000 RPM

70000 RPM   SHAFT DEFLECTION=0.025MM   MISALIGNMENT=0.0000RAD. 2-D MOTION
ROTATING DEFLECTION   STEADY MISALIGNMENT   MAX. ROLLER LOAD (N) = 960.

Roller E

Roller G   Roller F

Roller C

USOUT (M/S)

REVOLUTIONS

Figure 6. The Relative Slip Velocities Between the Rollers and the Outer Race Versus Time Measured in
           Revolutions of the Inner Race at 70,000 RPM

thus giving the negative relative slip velocity. When the cage impacts the roller as in the third event, (0.80 revolutions) the impact force is at the rear of the roller. This tends to accelerate the roller in the path about the center of the bearing, thus giving a positive relative slip velocity.

A measure of the overall skip in a high speed bearing is the deviation of the cage angular speed from the theoretical epicyclic cage angular speed. Figure 7 shows the variation of the cage angular speed as a ratio of the theoretical epicyclic speed. This ratio hovers near 0.87 (a cage slip of 13%) but still appears to be increasing, indicating that the new equilibrium has not yet been reached. The step changes correlate with the impact events described in the discussion of Figure 6.

The trajectory of the cage center is a measurable quantity in a test of an experimental bearing. The dynamics of the cage are very important in the design of a high speed bearing as the cage is the component which provides the coupling effects among the rollers. Figure 8 shows the trajectory of the cage center in a coordinate frame whose dimensions are in units of the radial clearance between the cage and the inner race guide flange.

Note that the cage has come in contact with the guide flange of the inner race at the bottom of the bearing near the dimensionless time of 1.2 revolutions. This should tend to accelerate the cage, but the effect is not easily discernible from Figure 7.

The cage-roller impact events presented in Figure 2 correlate with the abrupt changes in the cage center trajectory at the "knees" of the curve. The cage-roller impact exerts a radial force on the cage through the mechanism of rubbing traction between the cage and the roller in contact.

70000RPM   SHAFT DEFLECTION=0.025MM   MISALIGNMENT=0.0000RAD. 2-D MOTION
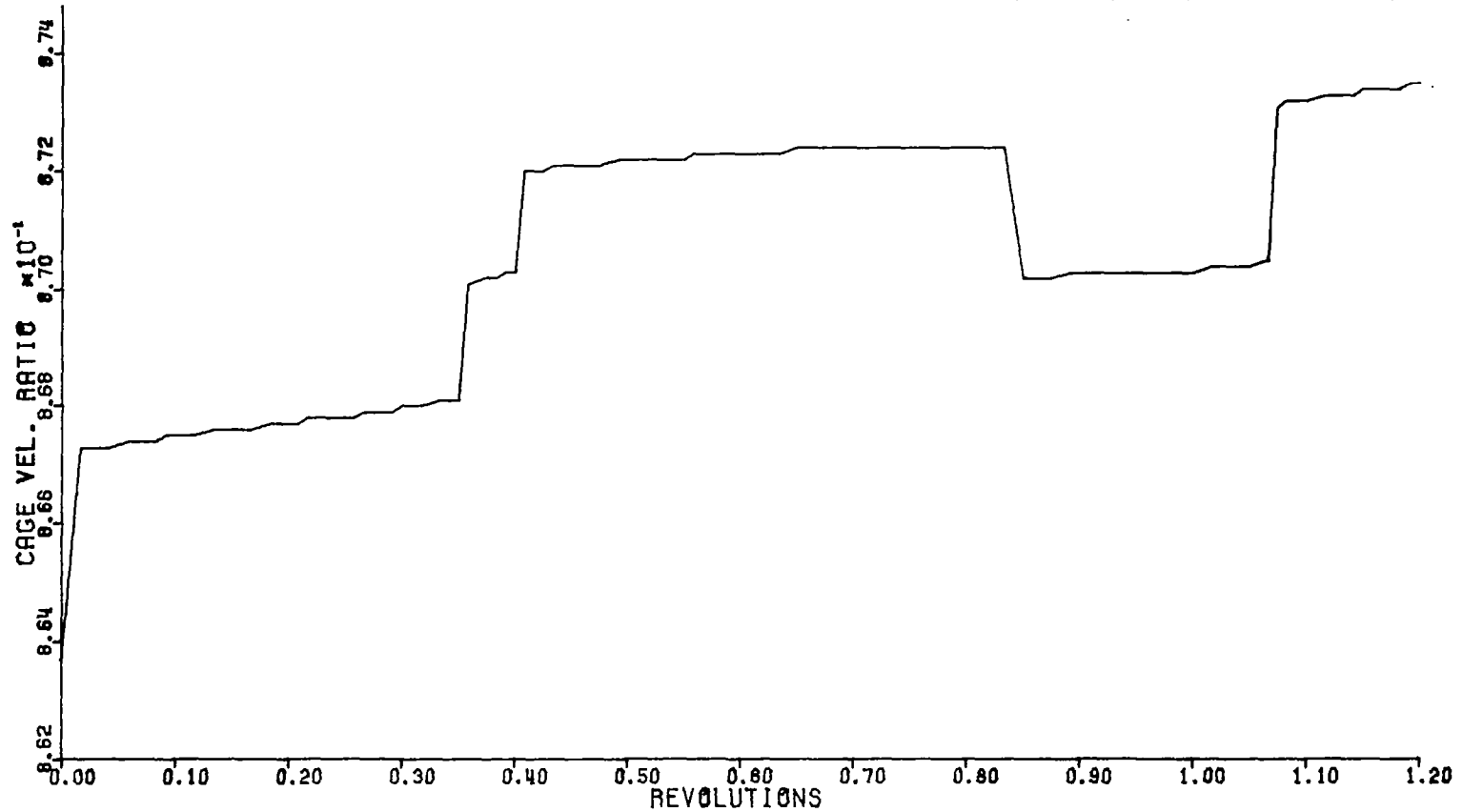ROTATING DEFLECTION   STEADY MISALIGNMENT   MAX. ROLLER LOAD (N)=960.

Figure 7.   The Ratio of the Cage Angular Speed to the Theoretical Cage Epicyclic Angular Speed Versus Time
Measured in Revolutions of the Inner Race at 70,000 RPM

2-D MOTION 70000RPM MAX. ROLLER LOAD (N)=960.
SHAFT DEFLECTION=0.025MM MISALIGNMENT=0.0000RAD.
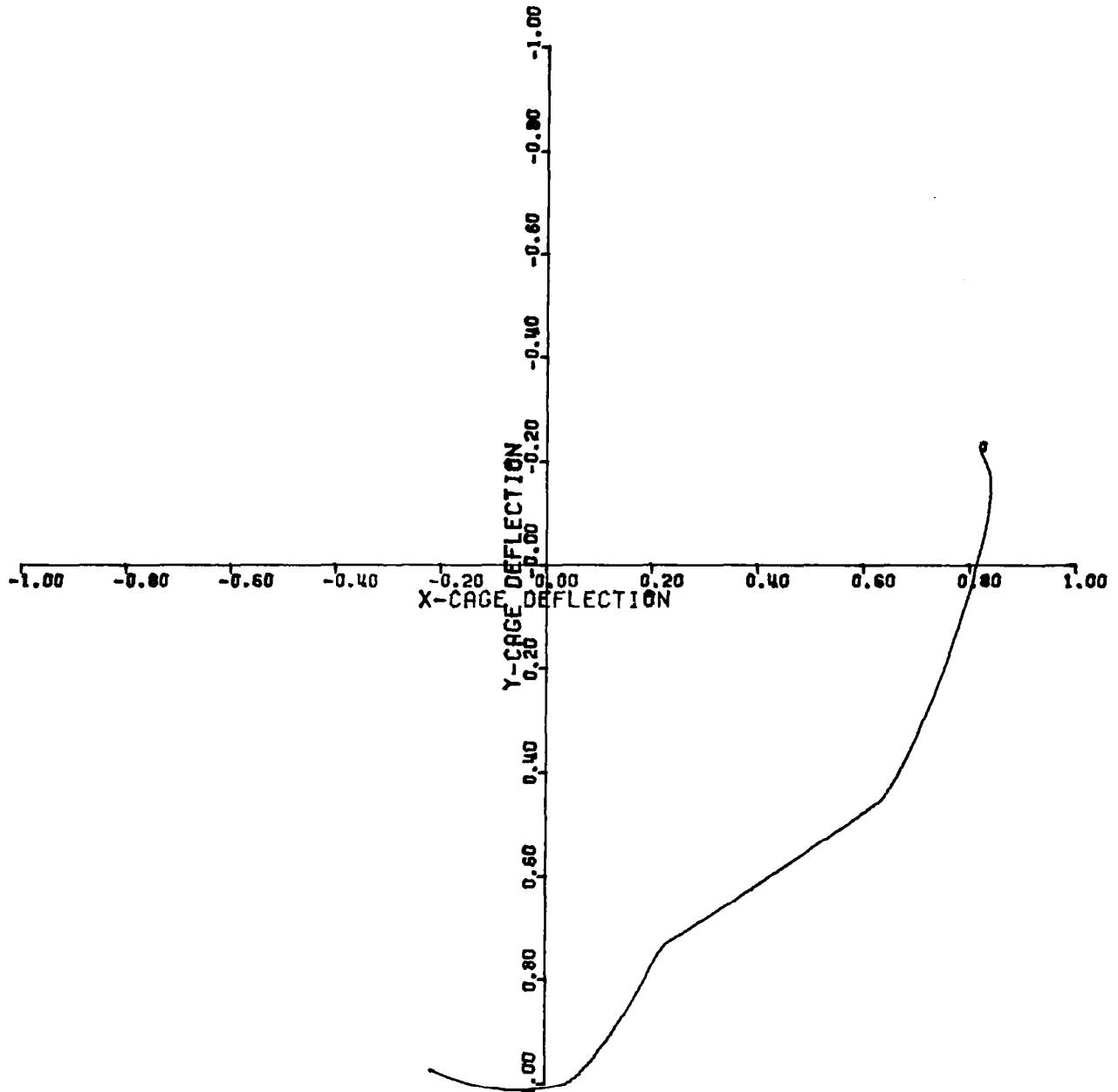ROTATING DEFLECTION   STEADY MISALIGNMENT

Figure 8. The Trajectory of the Cage Center Normalized with Respect to the Radial
Clearance Between the Cage and the Inner Race Guide Flange

30

Three Dimensional Simulation

The three-dimensional simulation initial conditions and loading parameters represent the effects of a suddenly applied steady misalignment and a sudden switch to a steady shaft deflection in the downward vertical direction from the rotating shaft deflection condition. The maximum roller load stayed constant at 591 N. Figures 9 through 14 indicate that the transient behavior due to the abrupt change in loading is completed by 0.20 revolutions. The general discussion of Figures 9 through 14 and Figure 18 parallels the discussion for Figures 2 through 8.

As it was for the two-dimensional simulation, the large values of FC (Fig. 9) correlate with abrupt changes in the USIN (Fig. 12), the USOUT (Fig. 13) and the cage velocity ratio (Fig. 14). The maximum impact force between a roller and the cage is (.171) (591) = 101 N (22.7 lb_f). This force corresponds to a maximum Hertz stress betweeen the cage pocket and roller A of 3.26×10^8 Pa (41,500 psi).

The loading applied in the three-dimensional simulation is steady, both for the radial deflection of the inner race relative to the outer race and for the misalignment of the inner race relative to the outer race. The load zone does not move in this case, thus a roller requires a dimensionless time of 0.6 revolutions of the inner race to traverse it as shown in Figure 10. Note too that the amount of misalignment is very small and does not induce a load zone between the inner race and rollers opposite to the load zone induced by the shaft deflection.

The magnitudes of the dimensionless traction forces, FIN and FOUT, in Figures 10 and 11 are comparable to those in Figures 3 and 4. The

31

70000 RPM   SHAFT DEFLECTION=0.020MM   MISALIGNMENT=0.0020RAD. 3-D MOTION
STEADY DEFLECTION   STEADY MISALIGNMENT   MAX. ROLLER LOAD (N) = 591.

Roller A

Roller E

Roller C
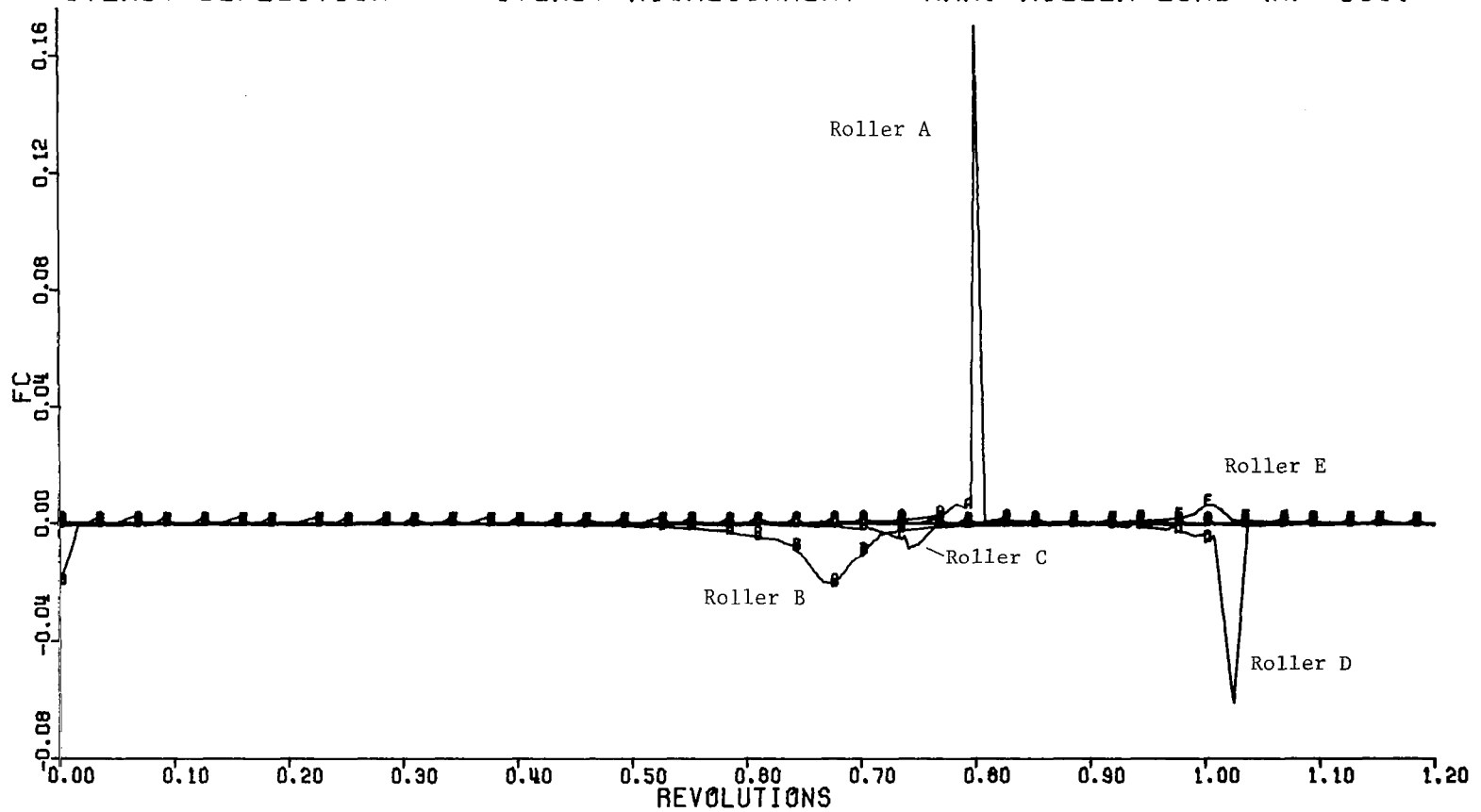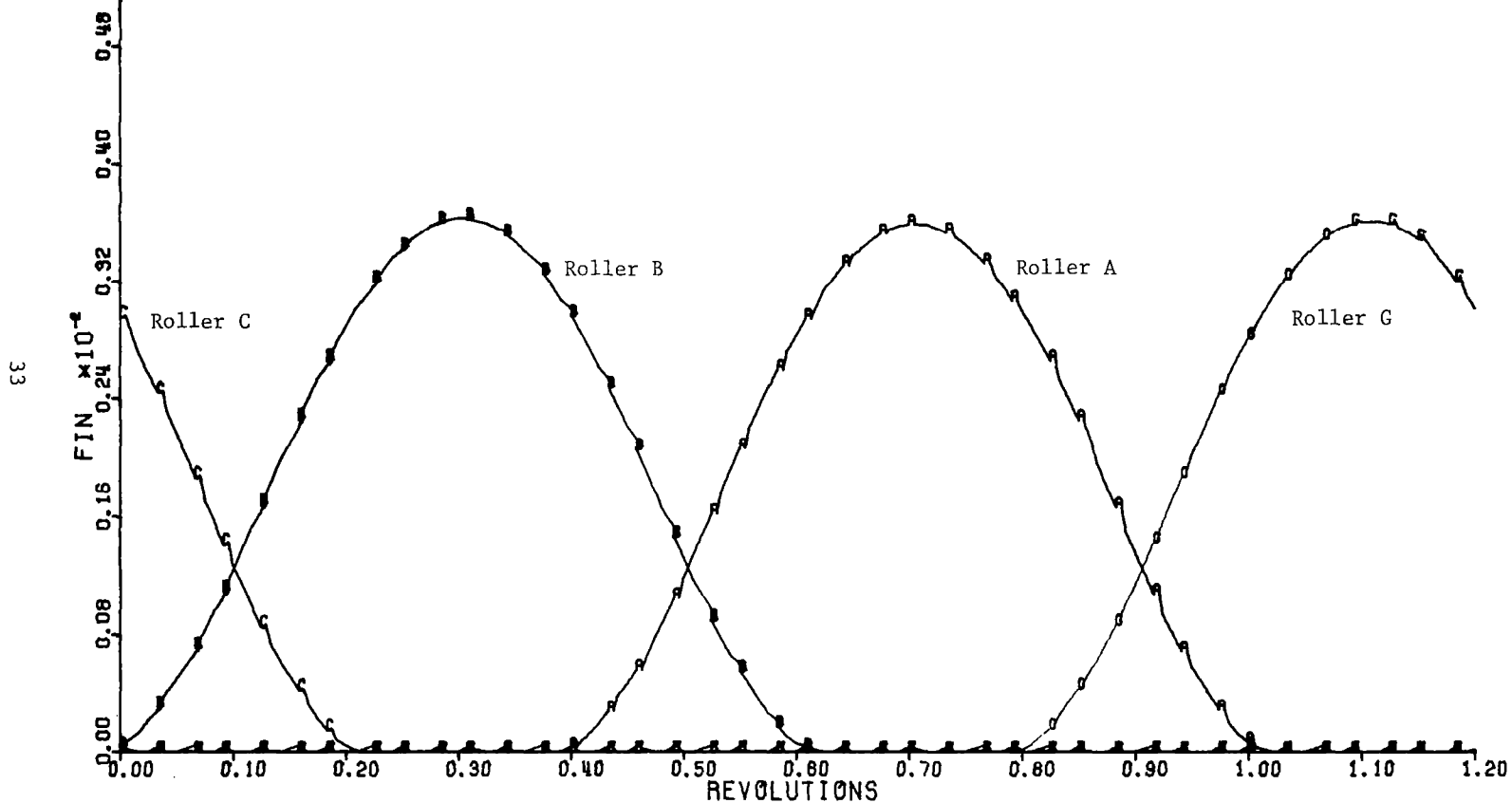
Roller B

Roller D

REVOLUTIONS

Figure 9.   The Dimensionless Normal Cage Forces Acting on the Rollers for the 3-D Simulation Versus Time
            Measured in Revolutions of the Inner Race at 70,000 RPM

70000RPM   SHAFT DEFLECTION=0.020MM   MISALIGNMENT=0.0020RAD. 3-D MOTION
STEADY DEFLECTION   STEADY MISALIGNMENT   MAX. ROLLER LOAD (N) = 591.

Figure 10. The Dimensionless EHD Traction Forces on the Rollers at the Inner Race for the 3-D Simulation
            Versus Time Measured in Revolutions of the Inner Race at 70,000 RPM

maximum value of the inner race/roller traction forces is about 2.1 N

(0.48 lb_f) due to the low normal forces between the rollers and the

inner race. The outer race/roller traction forces reach values of $(.05)$

$(591) = 29.5$ N (6.65 lb_f), Figure 11. The plots of FOUT in Figure 11

indicate that the dimensionless traction forces between the outer race

and the roller hover about zero (0 to 0.01). The large variations in

FOUT correlate to the rollers going through the load zone as shown in

Figure 10.

The relative slip velocities USIN and USOUT in Figures 12 and 13

have the same characteristics as the corresponding plots in Figures 5 and 6.

The values of USIN range from 12 to 16 m/s. The values of USOUT tend toward

zero except for the spikes shown at 0.75, 0.80 and 1.0 revolutions. These

events correlate with the cage to roller impacts shown in Figure 9.

The plot of the cage velocity ratio versus dimensionless time in units

of the revolutions of the inner race, Figure 14, remains close to 0.87.

This plot is similar to Figure 7 in that both indicate a very small rate

of increase in cage angular velocity and both show the sensitivity to cage-

roller impacts. The sharp increase and decrease in the cage velocity ratio

at 0.72 revolutions correlates with the cage/roller impacts shown in Fig-

ure 9.

The axial displacements of the rollers are plotted in Figure 15. The

initial conditions for all these displacements were zero. The rollers

which start to move axially are those which enter the load zone and are

subjected to the roller skew moment induced by the misalignment. The

rollers which pass through the total load zone, rollers B, A and G, are

displaced the farthest away from the center, reaching three-tenths of the
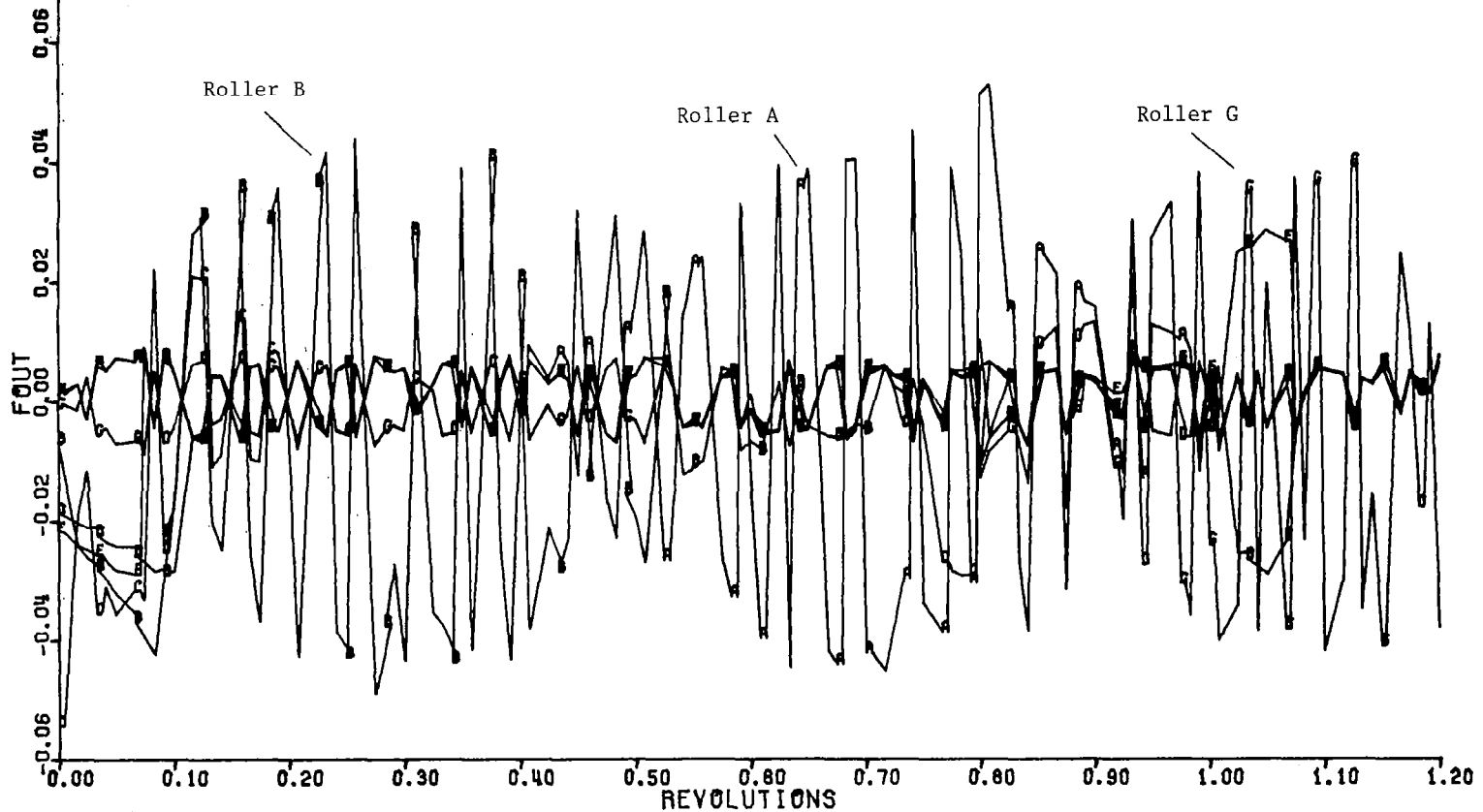
34

Figure 11a.   The Dimensionless EHD Traction Forces on the Rollers at the Outer Race for the 3-D Simulation Versus Time Measured in Revolutions of the Inner Race at 70,000 RPM

70000 RPM   SHAFT DEFLECTION=0.020MM   MISALIGNMENT=0.0020RAD. 3-D MOTION
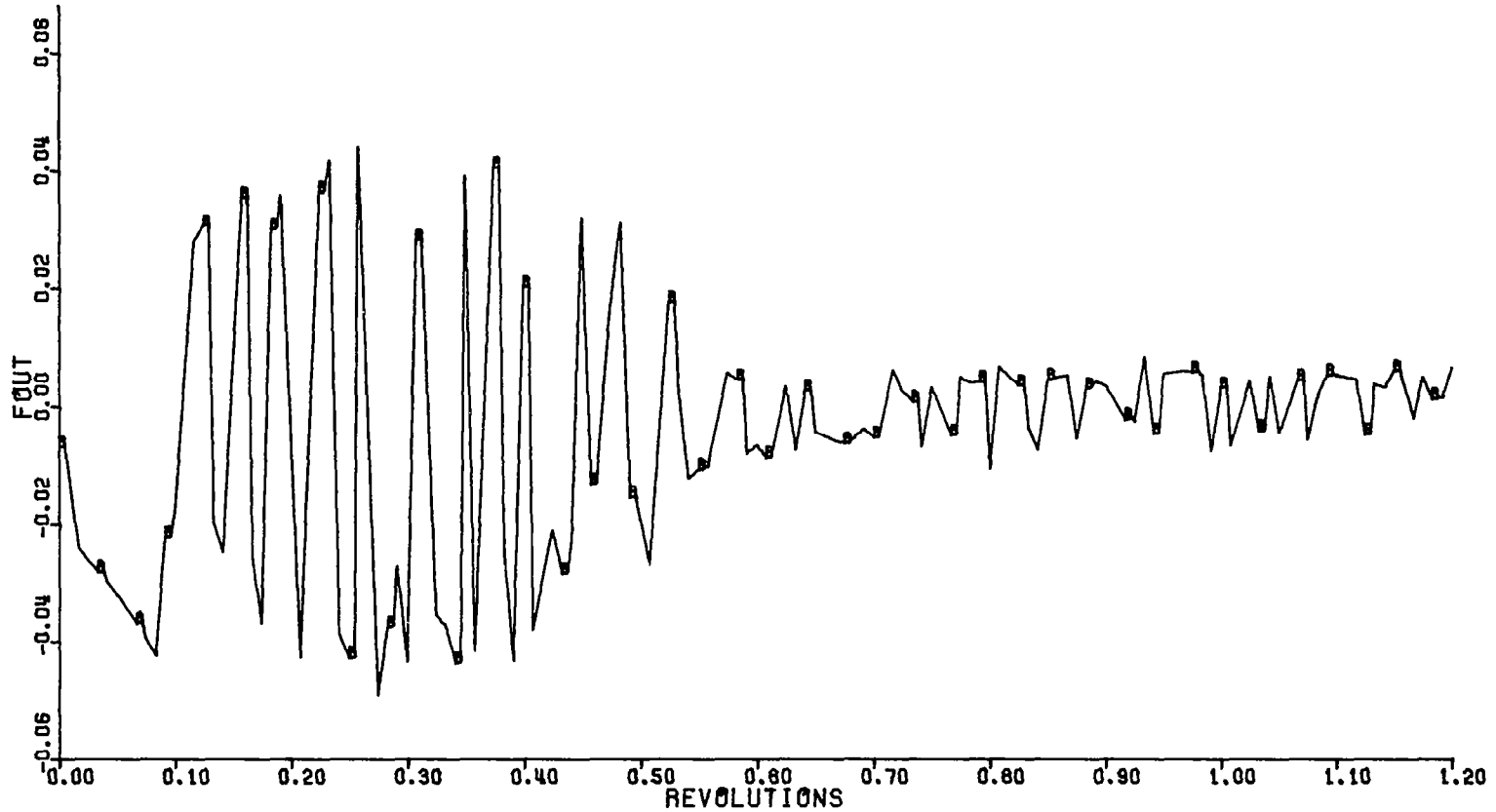STEADY DEFLECTION   STEADY MISALIGNMENT   MAX. ROLLER LOAD (N)=591.

Figure 11b.   The Dimensionless EHD Traction Force on Roller B at the Outer Race for the 3-D Simulation
Versus Time Measured in Revolutions of the Inner Race at 70,000 RPM

70000 RPM   SHAFT DEFLECTION=0.020MM   MISALIGNMENT=0.0020RAD. 3-D MOTION
STEADY DEFLECTION   STEADY MISALIGNMENT   MAX. ROLLER LOAD (N)=591.
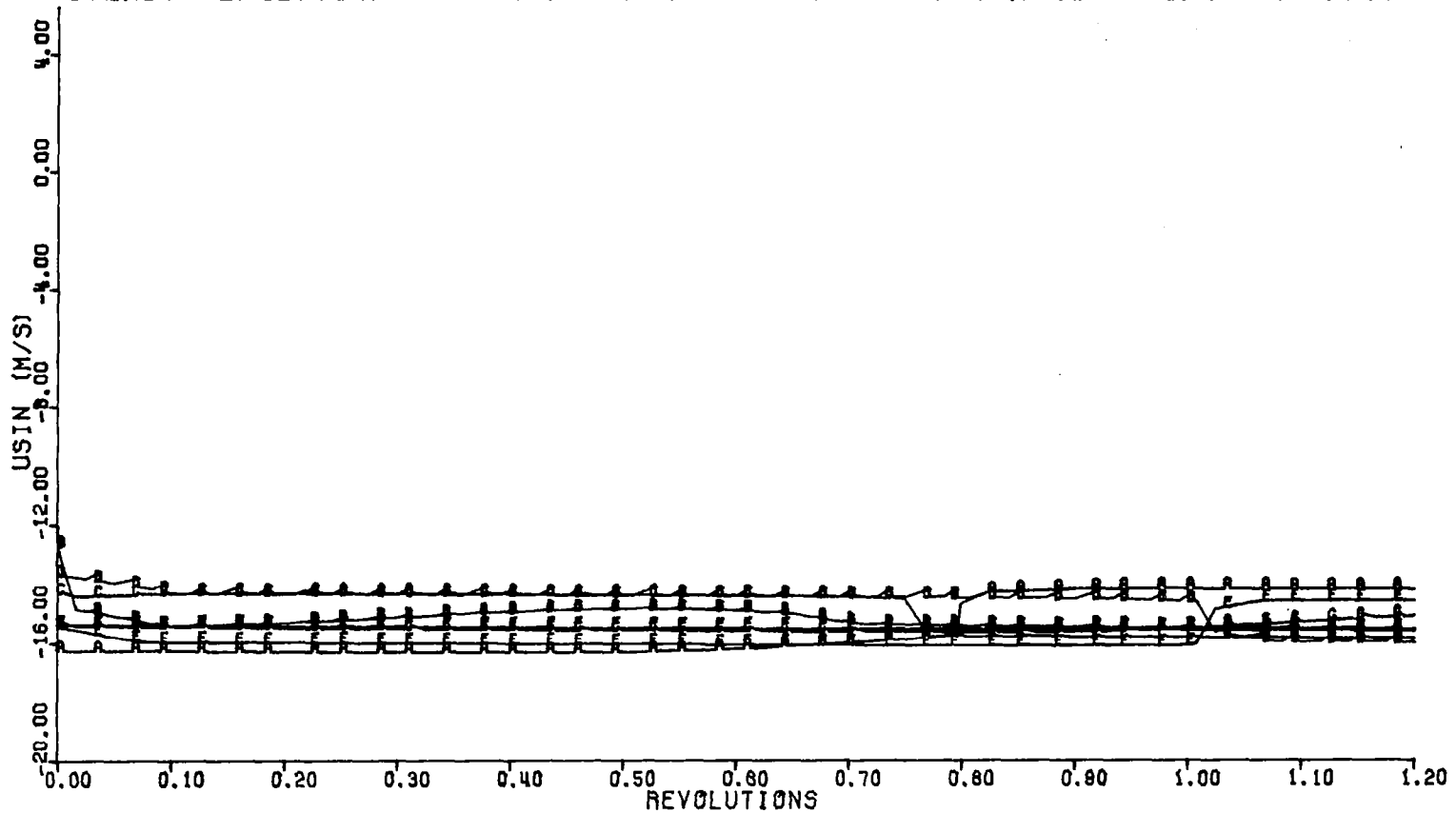

Figure 12.   The Relative Slip Velocities Between the Rollers and the Inner Race for the 3-D Simulation Versus
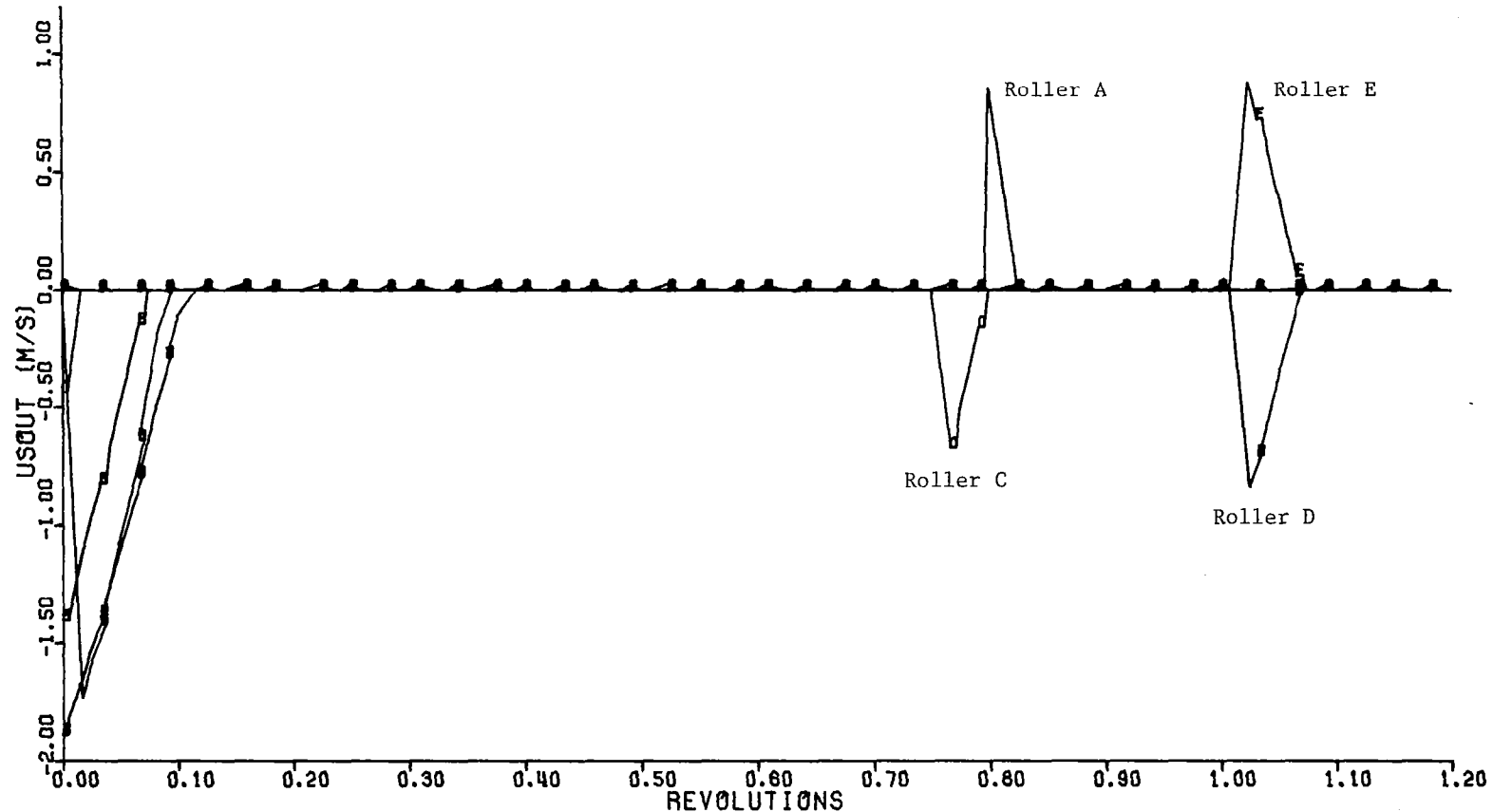Time Measured in Revolutions of the Inner Race at 70,000 RPM

Figure 13. The Relative Slip Velocities Between the Rollers and the Outer Race for the 3-D Simulation Versus Time Measured in Revolutions of the Inner Race at 70,000 RPM
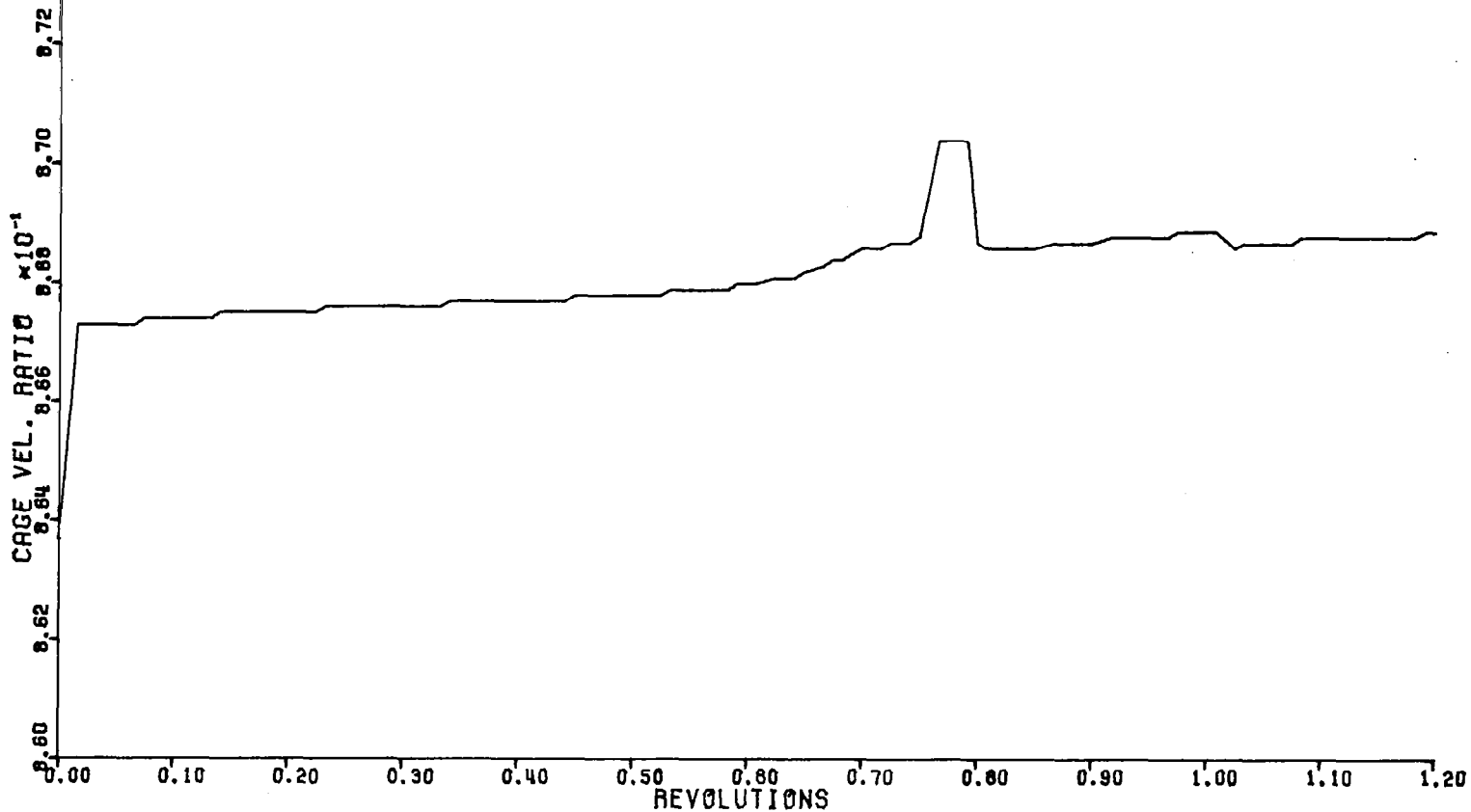
Figure 14. The Ratio of the Cage Angular Speed to the Theoretical Cage Epicyclic Angular Speed for the 3-D Simulation Versus Time Measured in Revolutions of the Inner Race at 70,000 RPM
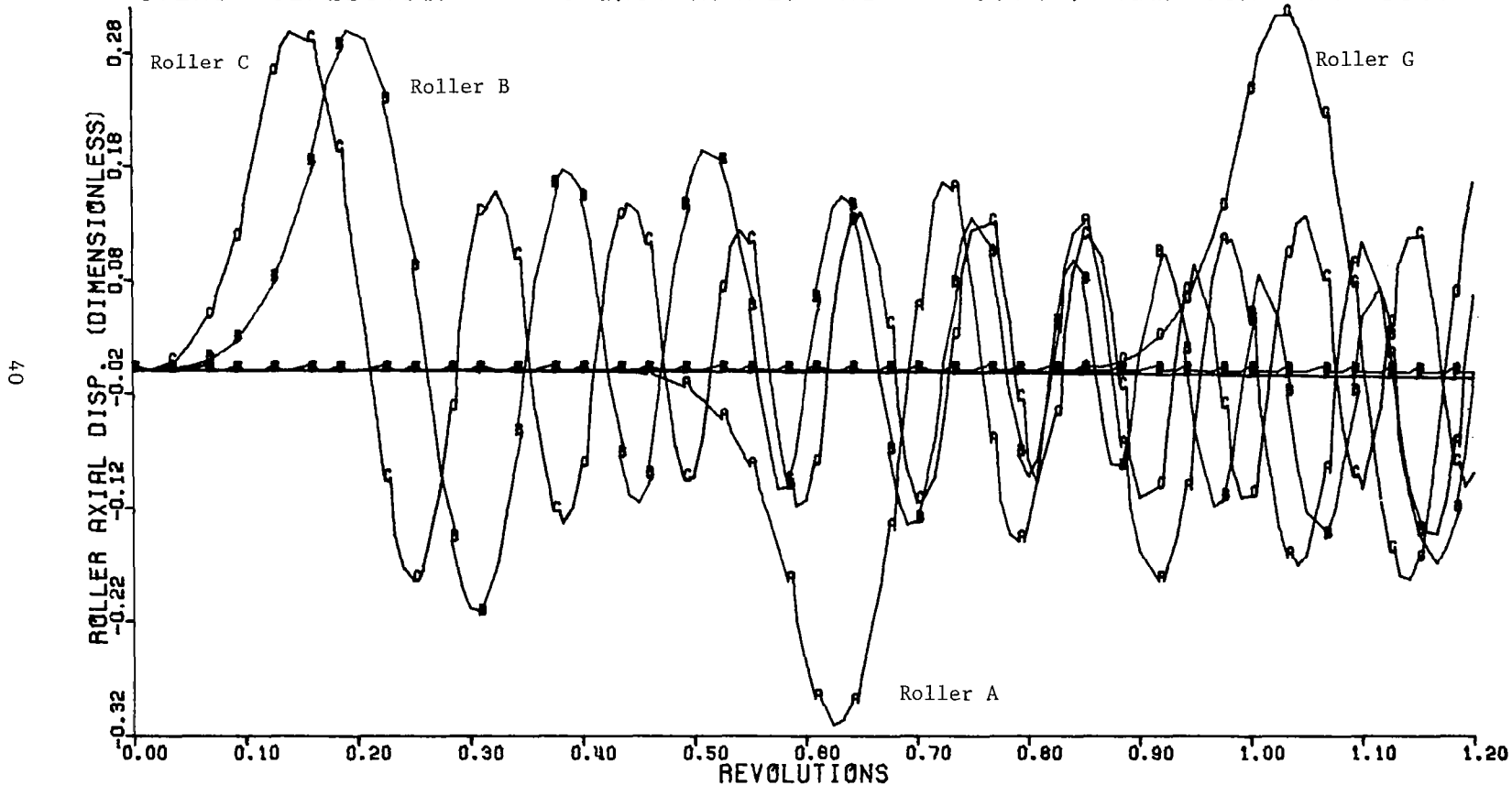
Figure 15. The Dimensionless Axial Displacement of the Rollers Versus Time Measured in Revolutions of the Inner Race at 70,000 RPM

total axial clearance between the roller ends and the inner race guide flanges.

The rollers are impacting the inner race guide flanges at discrete times during the 1.20 revolution period. As these events are of extremely short duration and are not continuous, it would be difficult to capture these data for plotting. A statement is printed by the computer program whenever the restoring torques due to the impact is nonzero, which permits the identification of the event time and magnitude.

The skew angles of the rollers are plotted in Figure 16. The magnitudes of the skew angles are small due to the very small axial clearance between the rollers and the inner race guide flanges. The skew angles fluctuate from positive to negative. This indicates that the rollers are exhibiting a "barrelling" motion as they move from side to side while orbiting in the bearing.

The dimensionless skew moment plotted in Figure 17 is always positive for this loading as the effect of the misalignment only presents itself in the primary load zone. The skew moments correlate to the loaded rollers as inferred from Figure 10. The sharp irregular curves are a result of subtracting the skew moment effect of the smoothly varying inner race traction forces from the skew moment effect of the irregular outer race traction forces, Figure 11.

The cage trajectory for the three dimensional simulation, Figure 18, has a different characteristic compared to the trajectory for the two dimensional simulation. The trajectory in Figure 18 is essentially a straight line until the cage impacts the inner race guide flange and changes direction near the bottom of the plot. The radial forces due to cage/roller

41

70000 RPM   SHAFT DEFLECTION=0.020MM   MISALIGNMENT=0.0020RAD. 3-D MOTION
STEADY DEFLECTION   STEADY MISALIGNMENT   MAX. ROLLER LOAD (N)=591.
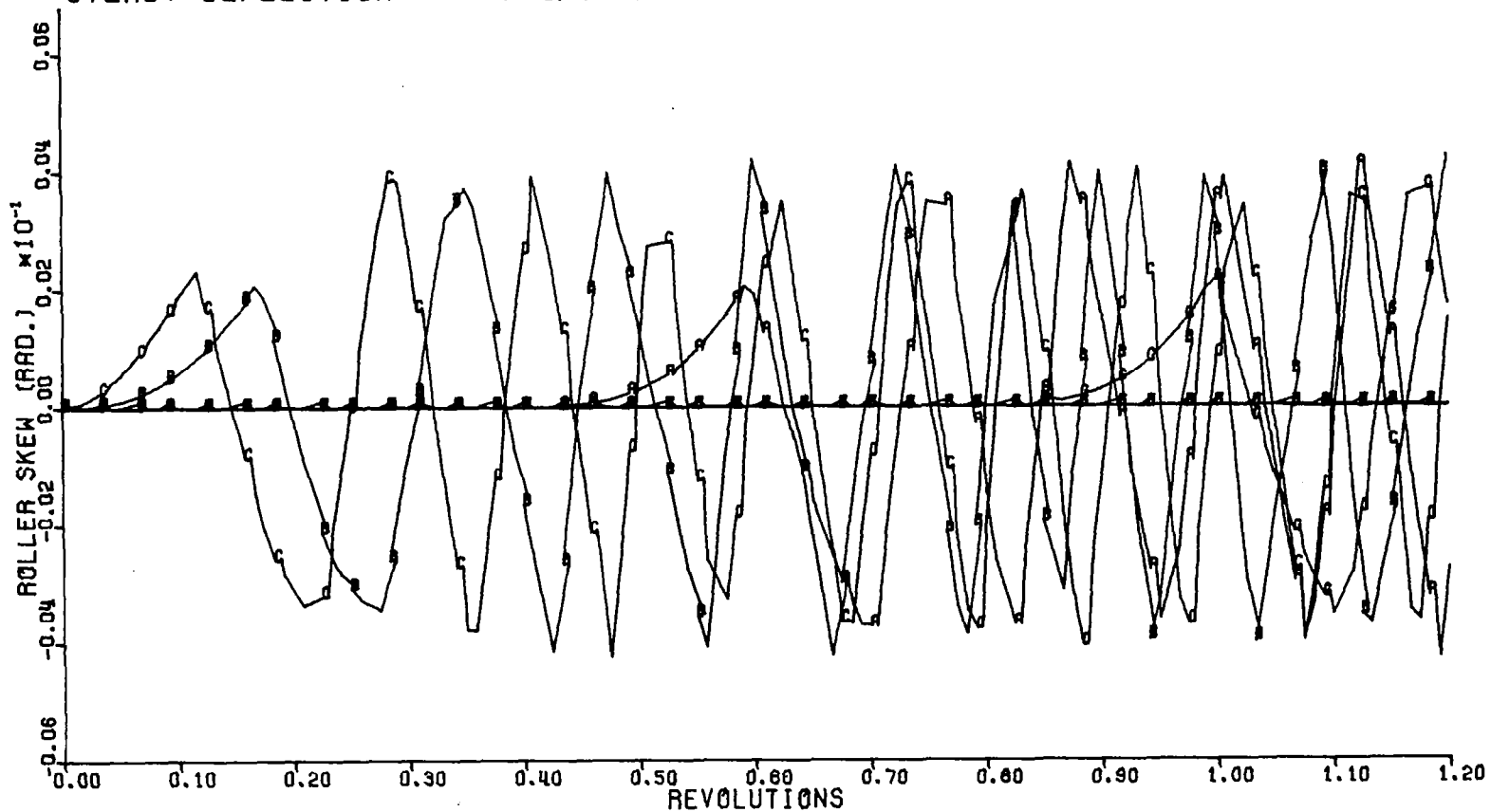
Figure 16.   The Skew Angle of the Rollers Versus Time Measured in Revolutions of the Inner Race at 70,000 RPM

70000 RPM   SHAFT DEFLECTION=0.020MM   MISALIGNMENT=0.0020RAD. 3-D MOTION
STEADY DEFLECTION   STEADY MISALIGNMENT   MAX. ROLLER LOAD (N)=591.

Roller B

Roller A

Roller G

SKEW MOMENT (DIMENSIONLESS) ×10⁻⁴

0.50
0.40
0.30
0.20
0.10
0.00
-0.10

0.00   0.10   0.20   0.30   0.40   0.50   0.60   0.70   0.80   0.90   1.00   1.10   1.20

REVOLUTIONS

43
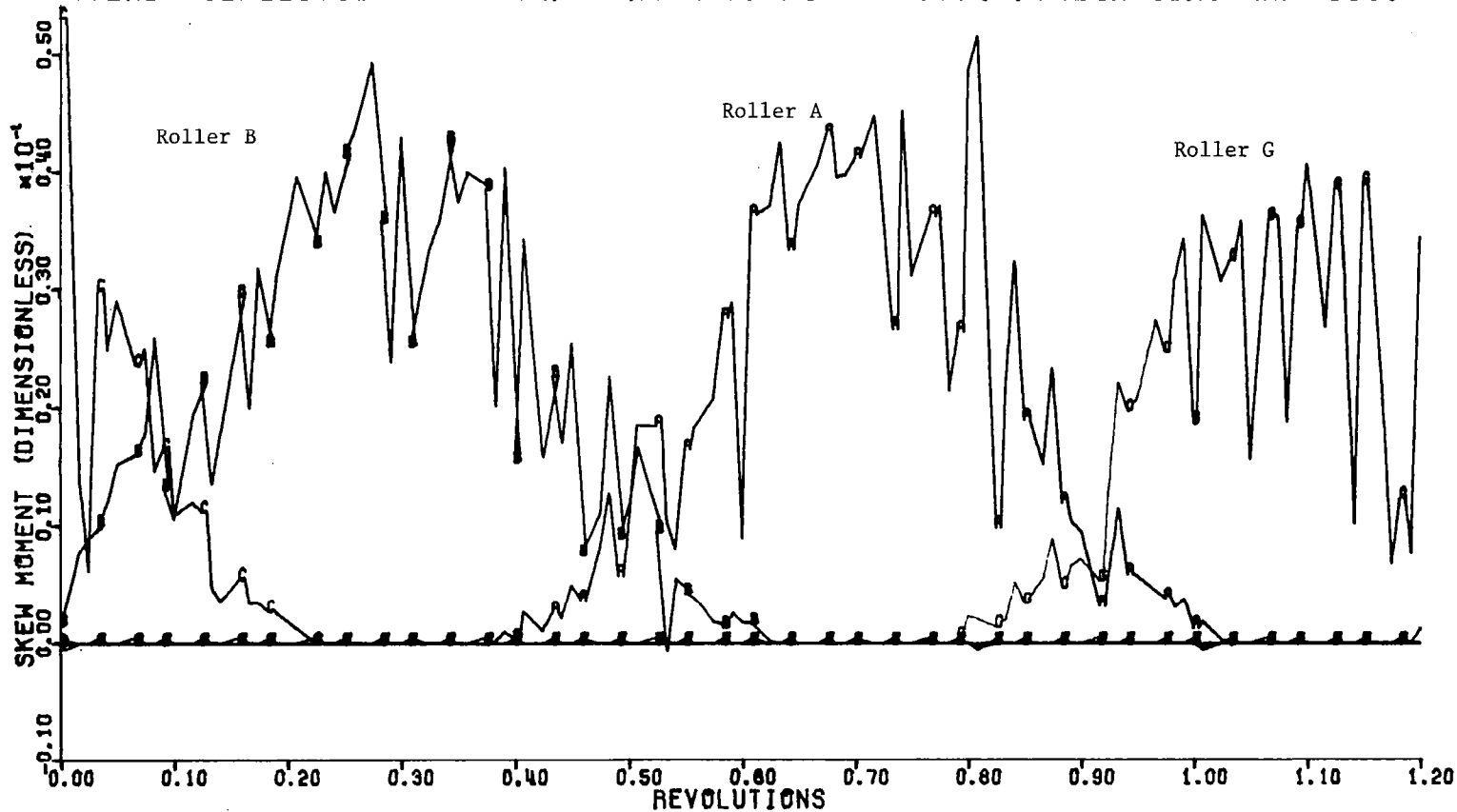
Figure 17a. The Dimensionless Skew Moment Acting on the Rollers Versus Time Measured in Revolutions of the
Inner Race at 70,000 RPM
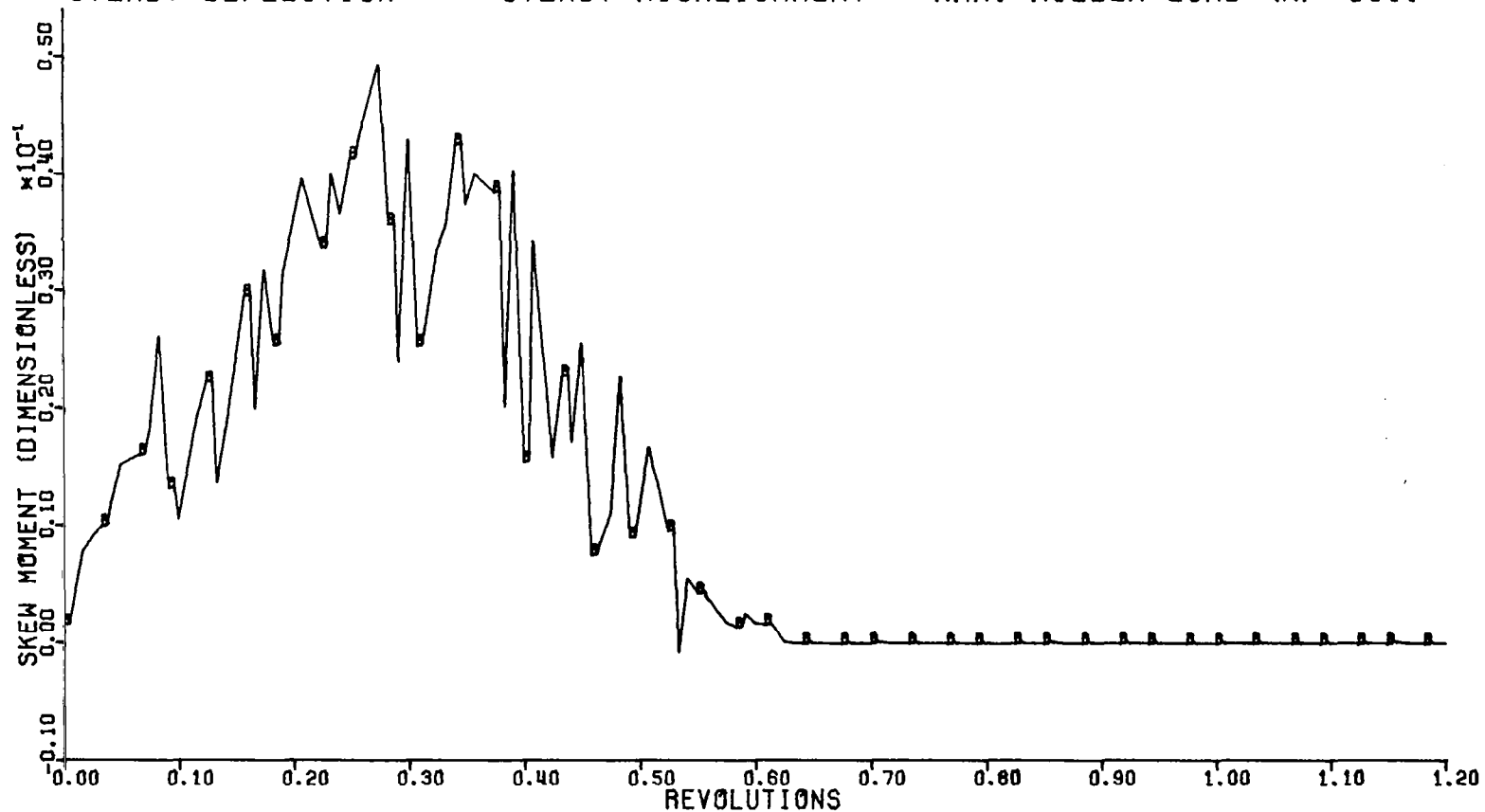
Figure 17b.   The Dimensionless Skew Moment Acting on Roller B Versus Time Measured in Revolutions of the
Inner Race at 70,000 RPM

3-D MOTION 70000RPM   MAX. ROLLER LOAD (N) = 591.
SHAFT DEFLECTION=0.020MM   MISALIGNMENT=0.0020RAD.
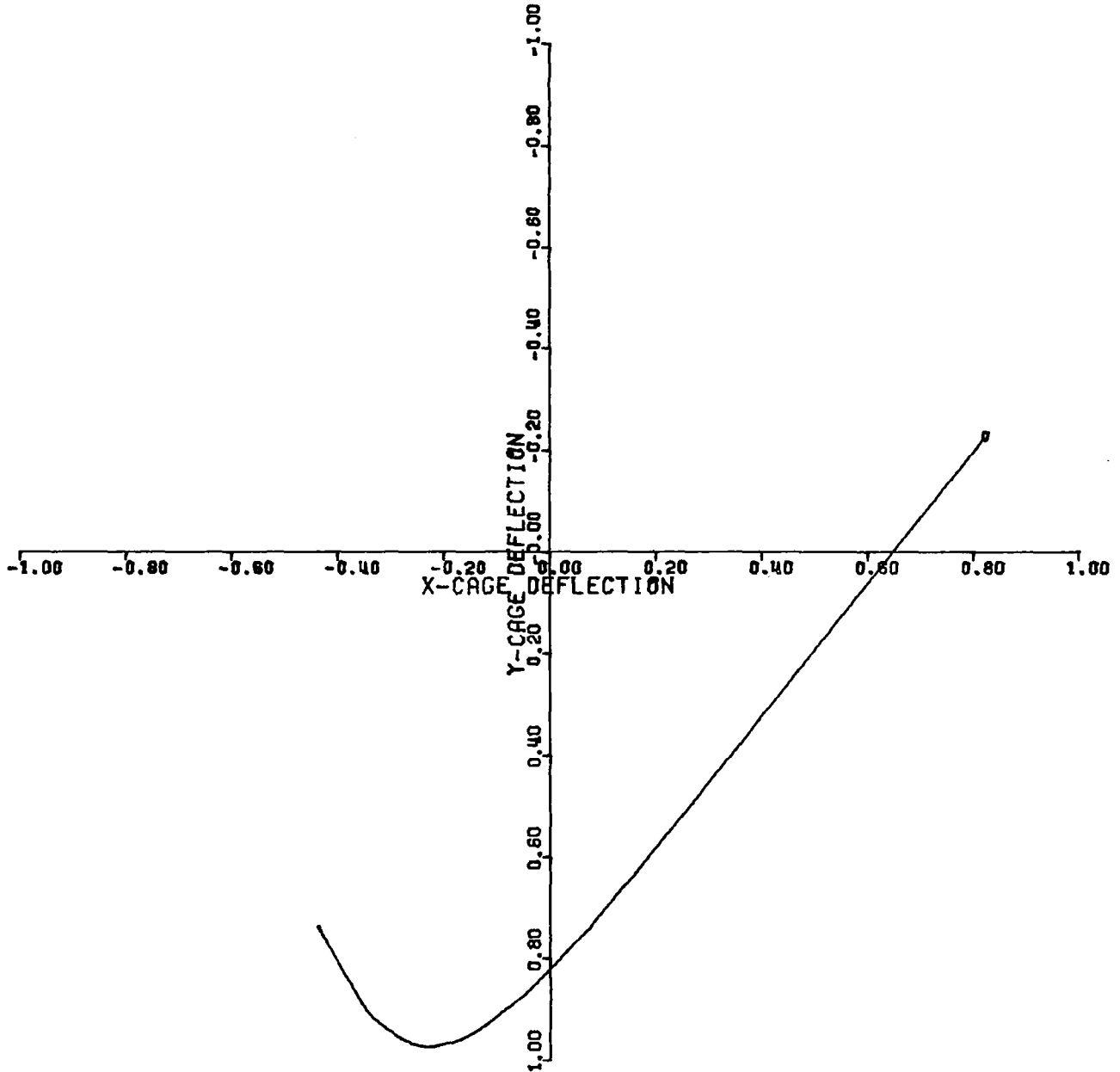STEADY DEFLECTION   STEADY MISALIGNMENT

Figure 18.   The Trajectory of the Cage Center Normalized with Respect to the
Radial Clearance Between the Cage and the Inner Race Guide Flange
for the 3-D Simulation

45

impact have a minor effect in this case as compared to Figure 8.

This discussion has shown that misalignment leads to roller skewing, that the roller regularly impacts the guiding flange and that roller/cage impacts can significantly affect the cage trajectory. In both the two-dimensional simulation and three-dimensional simulation, the slip velocities of the rollers at the inner race contact range between 12 and 16 m/s. The slip velocities of the rollers at the outer race contact stay close to zero. These effects are the result of the rollers trying to achieve force and torque equilibrium subject to relatively large forces at the outer race and relatively small forces at the inner race.

The results showing the effects of misalignment and roller/flange impacts are in agreement with Gupta [4]. Although two different bearings and operating conditions are being compared between this study and [4], the slip velocities at the inner and outer races appeared to be relatively constant whereas Gupta shows linearly varying slip velocities and a step change when load is removed from the contact. These trends observed in [4] do not agree with the trends observed in the present report.

One future modification which could be made to the computer program is a more detailed model for roller/flange interaction which would consider flange layback angle. The capability of specifying lubricant temperature at several key locations in the bearing would enhance the usefulness of the program and make it compatible with "steady state" dynamic simulation programs such as CYBEAN [11].

Future studies with this computer program should include a transient dynamic analysis of a production bearing which would include a parametric study of such important parameters as cage material, lubricant type, roller/cage clearances and diametral clearances. The effects of start up, speed changes, and shut down should also be included.

CONCLUDING REMARKS

A computer program for solving the nonlinear differential equations of motion of a high speed lightly loaded cylindrical roller bearing has been developed. This computer program has the capability of performing a two-dimensional or a three-dimensional simulation. Two example runs were presented to illustrate the use of the program and the plotted output. The computer program will be available through NASA.

REFERENCES

1. Conry, T. F., <u>Transient Dynamic Analysis of High-Speed Lightly Loaded Cylindrical Roller Bearings. I - Analysis</u>, NASA CR-3334, 1980.

2. Walters, C.T., "The Dynamics of Ball Bearings," <u>Journal of Lubrication Technology</u>, Trans. ASME, Series F, Vol. 93, no. 1 (1971) pp. 1-10.

3. Gear, C.W., <u>Numerical Initial Value Problems in Ordinary Differential Equations</u>, Prentice Hall (1971).

4. Gupta, P.K., "Dynamics of Rolling Element Bearings, Parts I to IV" <u>Journal of Lubrication Technology</u>, Trans. ASME, Vol. 101, no. 3 (1979) pp. 293-326.

5. Hindmarsh, A.C., "GEAR..Ordinary Differential Equation System Solver," UCID-30001, Rev. 3, Lawrence Livermore Laboratory, December 1974.

6. Harris, T.A., "The Effect of Misalignment on the Fatigue Life of Cylindrical Roller Bearings Having Crowned Rolling Members," <u>Journal of Lubrication Technology</u>, Trans. ASME, Vol. 91, Series F, no. 2 (1969) pp. 294-300.

7. Liu, J.Y., "The Effect of Misalignment on the Life of High Speed Cylindrical Roller Bearings," <u>Journal of Lubrication Technology</u>, Trans. ASME, Vol. 93, Series F, no. 1 (1971) pp. 60-68.

8. Dowson, D., Markho, P.H. and Jones, D.A., "The Lubrication of Lightly Loaded Cylinders in Combined Rolling, Sliding and Normal Motion, Part I: Theory," <u>Journal of Lubrication Technology</u>, Trans. ASME, Series F, Vol. 98, no. 4 (1976) pp. 509-516.

9. Palmgren, G., "Cylinder Compressed Between Two Plane Bodies," SKF Aktiebolaget Svenska Killagerfabriken, Goteborg, August 1949.

10. Rumbarger, J.H., Filetti, E.G. and Gubernick, D., "Gas Turbine Mainshaft Roller Bearing-System Analysis," Journal of Lubrication Technology, Trans. ASME, Series F, Vol. 95, no. 4 (1973) pp. 401-416.

11. Kleckner, R.J., Pirvics, J., Castelli, V., "High Speed Cylindrical Rolling Element Bearing Analysis 'CYBEAN' - Analytic Formulation," Journal of Lubrication Technology, Trans. ASME, Vol. 102, no. 3 (1980).

The input to the computer program may be classified into the cate-
gories of roller bearing geometry, material constants, operating speeds,
loading conditions, controls for the computations and output, and a set
of initial conditions. The input data deck for a two dimensional program
consists of 13+(NZ) cards, while the three dimensional program requires an
input data deck of 13+2(NZ) cards. The extra cards are needed to specify
the initial conditions for the additional 3(NZ) variables.

Card 1:   NZ, NPTS, NTYPE

Format: 3I5

   NZ   is the number of rollers.

   NPTS   is the number of slices in each roller which is used in the load

          distribution calculation.

   NTYPE is the code used to specify whether a two or three dimensional run

          will be made (2 or 3).

   The program has been dimensioned to accommodate 30 rollers and a cage
for the two dimensional problem or the three dimensional problem. If
larger problems are to be run, the dimension statements will have to be
changed.

Card 2:   E1, E2, E3, U1, U2, U3

Format: 6F10.6

   E1, E2, E3 are the moduli of elasticity of the inner race, roller and

          outer race respectively (psi).

   U1, U2, U3 are the Poisson's ratios of the inner race, roller and outer

          race respectively.

Card 3:   DRRACE, DRROLL, PD, ROLCLR, RADCOR, FLCOR

Format: 6F10.6

DRRACE   is the diameter of the inner race (in.).

DRROLL   is the diameter of the roller (in.).

PD   is the diametral clearance (in.).

ROLCLR   is half the total clearance between the roller ends and the
          inner race guide flange (in.).

RADCOR   is the corner radius of the roller (in.).

FLCOR   is the corner radius of the inner race guide flange (in.).

Card 4:   L, RCWN, ROLWGT, ROLDEN

Format: 3F10.6, E20.14

L   Is the axial length of the roller (in.).

RCWN   is the crown radius on the roller (in.).

ROLWGT   is the weight of a roller (lb_f).

ROLDEN   is the density of the roller material ($lb_f - sec^2/in^4$).

Card 5:   CGPOLR, CGDIA, CGWGT, CGLGH, CGCLR, CGPOC, CGHT

Format: E20.14, 6F10.6

CGPOLR   is the polar moment of inertia of the cage ($lb_f - in - sec^2$).

CGDIA   is the bore diameter of the cage (in.).

CGWGT   is the weight of the cage (lb_f).

CGLGH   is the face width of the cage next to one side of the inner
          race guide flange (in.).

CGCLR   is the radial clearance between the cage and the inner race
          guide flange (in.).

CGPOC   is the clearance between the roller and the cage pocket sides
          in the circumferential direction (in.).

51

CGHT   is the radial thickness of the cage (in.).

Card 6:   VISCCP, OILDEN, DECFUL

Format: 3F10.6

   VISCCP   is the absolute viscosity of the oil at operating temperature
             (centipoise).

   OILDEN   is the density of the oil (lb_m/in^3).

   DECFUL   is the ratio of the oil volume to the total volume in the bearing.

Card 7:   ANGDEF, OMANDF, SHDEF, OMSHDF

Format: 5F10.6

   ANGDEF   is the total angular misalignment between the shaft and the
             outer race (radians).

   OMANDF   is the control variable for steady angular deflection about the
             x axis (0), angular deflection rotating at shaft speed WS(+1), or
             steady angular deflection about the y axis (-1). (See Fig. 1 [1])

   SHDEF   is the total shaft linear deflection relative to the outer race
             support (in.).

   OMSHDF   is the control variable for steady linear deflection in the +y
             direction (-1) or a linear deflection rotating at shaft speed
             WS(+1).

Card 8:   WMXRPM

Format: F10.1

   WMXRPM   is the maximum shaft speed (rev/min).

Card 9:   H, T, TBND, TSPACE

Format: 4F10.8

   H   is the starting step size for numerical integration (dimension-
             less time). Refer to eqn (73) Part I [1]. Choose a value of
             0.0002. If it is too large or too small, the integration program,
             GEAR, will adjust the step size.

T is the initial value of dimensionless time

TBND is the final value of dimensionless time

TSPACE is the interval of dimensionless time at which the vector of
dependent variables is printed.

Card 10: TPLT

Format: F10.8

TPLT is the interval of dimensionless time at which the quantities
of interest are placed into a file to be plotted.

Card 11: Y(1), Y(2), Y(3)

Format: 3D20.10

Y(1) is the initial velocity of the cage in the x direction non-
dimensionalized by the theoretical epicyclic speed (eqn. 3) and the
radial clearance.

Y(2) is the initial displacement of the cage in the x direction in
units of the radial clearance between the cage and the inner
race guide flange.

Y(3) is the initial velocity of the cage in the y direction non-
dimensionalized by the theoretical epicyclic speed and the
radial clearance.

Card 12: Y(4), Y(5), Y(6)

Format: 3D20.10

Y(4) is the initial displacement of the cage in the y direction in
units of the radial clearance between the cage and the inner
race guide flange.

Y(5) is the initial angular velocity of the cage nondimensionalized
by the theoretical epicyclic speed.

Y(6)   is the initial angular position of the cage (radian).

Card 13 through Card 12+NZ: Y(J), Y(J+1), Y(J+2)

Format: 3D20.10

   where J=7, 10, 13, ..., 4+3(NZ)

   Y(J)   is the initial relative velocity between the i 'th roller

            [J=4+3i] and the cage nondimensionalized by the clearance

            (CGPOC) and the theoretical epicyclic speed.

   Y(J+1)   is the initial relative displacement between the i 'th roller

            and the cage nondimensionalized by the clearance (CGPOC).

   Y(J+2)   is the initial angular velocity of the roller about its own

            axis nondimensionalized by the theoretical epicyclic speed.

Card 13+NZ: FORDIM, OMTHEO

Format: 3D20.10

   FORDIM   is the force F* used in determining the time scaling. It is

            set to zero and determined internally for new runs. When the

            program is restarted, this is the value utilized in the pre-

            vious run (1b$_f$).

   OMTHEO   is the theoretical angular velocity used in determining the

            time scaling. It is normally set to zero for new runs. When

            the program is restarted, this is the value utilized in the

            previous run (rad/sec).

The data cards described above are for a two dimensional run (NTYPE=2).

If a three dimensional run were to be made, NZ data cards would have to

be inserted between Card 12+NZ and Card 13+NZ given above. The other data

cards would remain the same.

Card 13+NZ through Card 12+2(NZ): Y(K), Y(K+1), Y(K+2)

Format: 3D20.10

  where   K=3(NZ)+7, 3(NZ)+10, ..., 6(NZ)+4

  Y(K)   is the initial angular velocity of skew of the i 'th roller

            [K=4+3(NZ)+3i].   It is nondimensionalized by the theoretical

            epicyclic speed.

  Y(K+1)   is the initial angle of skew of the roller (radian).

  Y(K+2)   is the initial axial displacement of the roller.   It is non-

            dimensionalized on the total clearance between the roller ends

            and the guide flanges (2·ROLCLR).

     The card with FORDIM and OMTHEO is always the last card in the data

deck.

APPENDIX B

PROGRAM OUTPUT

The printed output is written on unit 6 at an interval specified in the input data. The state variables and other data needed to restart the program are written onto a unit labeled JDATA. In this program JDATA is unit 10. Most of the interesting output data are not the dependent variables themselves, but such quantities as the traction forces between the rollers and the races or the slip velocities between the rollers and the races. These data, which are to be plotted, are written on a unit labeled JPLT, and are also plotted by the program. In this program JPLT is unit 9.

After the differential equation solver has numerically integrated the differential equations to TBND, the program will stop. The last data to be written on the unit JDATA are a set of card images containing all the input data on the first ten cards as described above with the exception of the ninth card where the entry for T is replaced by the final value of dimensionless time attained by the program. The initial conditions as described above are replaced by the values of the dependent variables at the final value of dimensionless time. The last card image contains the values of FORDIM and OMTHEO used in the computation.

To restart the program using these card images, a new value of TBND must be inserted such that TBND is greater than T. This new set of data allows the user to examine the output of the program in stages and, if it appears to be functioning properly, to allow the program to continue.

The plot data stored on the unit labeled JPLT can then be transferred to a program which controls the plotting routines. Every computer

56

has its own specific library of plotting·routines so the most general way of presenting the output data is to store it in a data file and adapt it to an available computer system and software. A subroutine, PLODAT, is used to plot the data on the University of Illinois CYBER 175.

The data is stored in blocks on unit JPLT. The first line of each block has the counter value associated with that block, IPLT, the time in units of shaft revolutions, PTREV, the x and y positions of the center of the cage scaled on the radial clearance between the cage and the inner race guide flange, PXCG and PYCG, and the angular speed of the cage scaled on the theoretical cage epicyclic speed, PCGV. The format used for this line is (I 10, 7 E 10.4).

The remaining data in the block is given, for each roller, as:

The cage-roller interaction force on the roller scaled by F*.

```
FC(J), J=1,NZ
FORMAT (8E10.4)
```

The traction force on the roller at the inner race contact scaled by F*.

```
FIN(J), J=1,NZ
FORMAT (8E10.4)
```

The traction force on the roller at the outer race contact scaled by F*.

```
FOUT(J), J=1,NZ
FORMAT (8E10.4)
```

The relative sliding velocity between the roller and the inner race in (m/sec),

57

```
                 USIN(J), J=1,NZ
                 FORMAT (8E10.4)
```

The relative sliding velocity between the roller and the inner race in (m/sec),

```
                 USOUT(J), J=1,NZ
                 FORMAT (8E10.4)
```

The following data are also plotted for the three dimensional problem:

The roller skew angle in units of radians,

```
                 Y(J), J=3*NZ+8, 6*NZ+5, 3
                 FORMAT (8E10.4)
```

The roller axial displacement scaled on the total axial clearance between the roller and the cage pocket,

```
                 Y(J), J=3*NX+9, 6*NZ+6, 3
                 FORMAT (8E10.4)
```

The skewing torque on the roller induced by non symmetrical EHD traction forces on the roller scaled by the product $I_t \omega_e^2$, where I_t is the transverse moment of inertia of the roller and ω_e is the inverse of the characteristic time associated with the scaling force F*.

```
                 ROLMOM(J), J=1,NZ
                 FORMAT (8E10.4)
```

1. Report No. NASA CR-3335	2. Government Accession No.	3. Recipient's Catalog No.
4. Title and Subtitle TRANSIENT DYNAMIC ANALYSIS OF HIGH-SPEED LIGHTLY LOADED CYLINDRICAL ROLLER BEARINGS II - COMPUTER PROGRAM AND RESULTS		5. Report Date January 1981
		6. Performing Organization Code
7. Author(s) Thomas F. Conry and Peter R. Goglia		8. Performing Organization Report No. None
		10. Work Unit No.
9. Performing Organization Name and Address University of Illinois at Urbana-Champaign Urbana, Illinois		11. Contract or Grant No. NSG-3098
		13. Type of Report and Period Covered Contractor Report
12. Sponsoring Agency Name and Address National Aeronautics and Space Administration Washington, D.C. 20546		14. Sponsoring Agency Code

15. Supplementary Notes

Lewis Technical Monitor: Harold H. Coe
Final Report

16. Abstract

The governing differential equations of motion for a high speed cylindrical roller bearing are programmed for numerical solution and plotted output. This computer program has the capability of performing a two-dimensional or three-dimensional simulation. Two numerical solutions of the governing differential equations were obtained to simulate the motion of a roller bearing, one for the two-dimensional equations of motion and one for the three-dimensional equations of motion. Computer generated plots were obtained and present such data as roller/cage interaction forces, roller/race traction forces, roller/race relative slip velocities and cage angular speed over a non-dimensional time equivalent to 1.2 revolutions of the inner race. Roller axial displacement, roller skew angle and skew moment are also plotted for the three-dimensional solution. The trajectory of the cage center is plotted for both the two-dimensional and three-dimensional solutions.

17. Key Words (Suggested by Author(s)) Computer program Cylindrical roller bearing Analysis Dynamic analysis	18. Distribution Statement Unclassified - unlimited Subject Category 37		
19. Security Classif. (of this report) Unclassified	20. Security Classif. (of this page) Unclassified	21. No. of Pages 61	22. Price* A04